SISTEMAS DINÁMICOS Y COSMOLOGÍA
XXX CONGRESO DE MATEMÁTICAS CAPRICORNIO
COMCA 2022

Genly Leon Torres

Departamento de Matemáticas
Universidad Católica del Norte

August 3-5, 2022

Contents

Universidad Católica del Norte ver más allá

XXX CONGRESO DE MATEMÁTICA CAPRICORNIO COMCA 2022

2

1. Applications of dynamical systems in Cosmology
   (a) Scalar field cosmology
2. Static LRS class II spacetimes sourced by a scalar field
   (a) Massless scalar field
   (b) Exponential Potential
   (c) Arbitrary Potential
   (d) Martinez-Troncoso-Zanelli (MTZ) black hole

Universidad Católica del Norte
ver más allá

XXX CONGRESO DE MATEMÁTICA CAPRICORNIO
COMCA 2022

Dynamical systems in cosmology

In dynamical systems, phase space is a space in which all possible states of a system are represented. In phase space, every degree of freedom or parameter of the system is represented as an axis of a multidimensional space; a one-dimensional system is called a phase line, while a two-dimensional system is called a phase plane.

- Let $\mathcal{M}$ be the class of all cosmological models whose state at time t can be represented as an element $\mathbf{x}$ in an state space Σ.
- The evolution of an element of the class Σ is determined by the solution of a system of equations differential with constraints

$$\partial_t \mathbf{x} = \mathbf{X}(\mathbf{x}, \partial_i \mathbf{x}, \ldots), \ \mathbf{C}(\mathbf{x}, \partial_i \mathbf{x}, \ldots) = \mathbf{0} \tag{1}$$

where ∂_i denotes partial derivative with relation to x^i, and $\ldots$ denotes possible higher-order derivatives.

- For homogeneous cosmologies, (1) reduces to

$$\frac{\mathrm{d}y}{\mathrm{d}\tau} = f(y), \quad y \in \mathbb{R}^n, \quad g(y) = 0, \tag{2}$$

Procedure

1. Determine when the state space defined by (2), it is compact.
2. Identify lower dimensional invariant sets, which contain orbits of model classes with additional symmetries.
3. Find all singular points and analyse their local stability. Find its stable and unstable manifolds, which can coincide with some of the invariant sets found in point (2).
4. Find Dulac functions or monotonic functions defined in as many invariant sets as possible.
5. Investigate bifurcation of parameters. The bifurcations may be associated with changes in the local stability of the singular points.
6. With all the information contained in (1) - (5) you can make precise guesses about the asymptotic evolution. The monotonic functions in point (4), combined with theorems of the theory of dynamical systems, can allow to prove those conjectures.
7. Knowing the stable and unstable manifolds of singular points, it is possible to construct all possible heteroclinic sequences that join the attractor of the past with the attractor of the future, allowing to obtain information about the intermediate behaviour's of the models.

5

1. Use dynamical systems theory to determine the asymptotic states of cosmological models, particularly when the governing equations are a finite system of autonomous ordinary differential equations.
2. Discuss cosmological models as dynamic systems, with special emphasis on applications in the early Universe.
3. Review the asymptotic properties of spatially homogeneous and inhomogeneous models in general relativity.
4. Discuss the results related to scalar field models with an exponential potential (with and without barotropic matter).
5. Discuss the dynamic properties of cosmological models derived from effective actions.
6. Use computational tools to solve problems.

Universidad Católica del Norte ver más allá
XXX CONGRESO DE MATEMÁTICA CAPRICORNIO COMCA 2022

1. Within general relativity (GR):

Model	Lagrangian Density	Eqs. of Motion
Quintessence	$\mathcal{L}_\phi = -V(\phi) + X$	$\ddot{\phi} + 3H\dot{\phi} + \frac{dV}{d\phi} = 0$
Tachyon	$\mathcal{L}_\phi = -V(\phi)\sqrt{1-2X}$	$\frac{\ddot{\phi}}{1-\dot{\phi}^2} + 3H\dot{\phi} + \frac{1}{V}\frac{dV}{d\phi} = 0$
Phantom	$\mathcal{L}_\phi = -V(\phi) - X$	$\ddot{\phi} + 3H\dot{\phi} - \frac{dV}{d\phi} = 0$
K-essence	$\mathcal{L}_\phi = L(\phi, X)$ L non-linear in X	$\left(\frac{\partial L}{\partial X} + 2X\frac{\partial^2 L}{\partial X^2}\right)\ddot{\phi} + \frac{\partial L}{\partial X}(3H\dot{\phi}) + \frac{\partial^2 L}{\partial\phi\partial X}\dot{\phi}^2 - \frac{\partial L}{\partial\phi} = 0$

where $X \equiv -\frac{1}{2}g^{\alpha\beta}\partial_\alpha\phi\partial_\beta\phi$

2. Modified gravity (GM): scalar-tensor and $f(R, R_{ab}R^{ab}, \ldots)\ldots$ theories.

Consider now as a candidate for dark energy a quintessence scalar field with action $S_\phi = \int dx^4 \sqrt{-g} \left(-\frac{1}{2} g_{\mu\nu} \phi^{;\mu} \phi^{;\nu} + V(\phi) \right)$ and an ideal gas, The field equations comprise the set of differential equations,

$$-3a\dot{a}^2 + \frac{1}{2} a^3 \dot{\phi}^2 + a^3 V(\phi) = a^3 \rho_m, \tag{3}$$

$$\ddot{a} + \frac{1}{2a} \dot{a}^2 + \frac{a}{2} \dot{\phi}^2 - aV(\phi) = -w_m a \rho_m, \tag{4}$$

where the scalar field, $\phi(t)$, satisfies the equation

$$\ddot{\phi} + \frac{3}{a} \dot{a} \dot{\phi} + V(\phi)_{,\phi} = 0. \tag{5}$$

We define $H = \frac{\dot{a}}{a}$ which is the Hubble function, with value today H_0 which is the Hubble constant.

Universidad Católica del Norte ver más allá

XXX CONGRESO DE MATEMÁTICA CAPRICORNIO COMCA 2022

With the use of the Hubble function, the field equations becomes

$$\begin{aligned} 3H^2 &= \frac{1}{2}\dot{\phi}^2 + V(\phi) + \rho_m, & (6) \\ -2\dot{H} - 3H^2 &= \frac{1}{2}\dot{\phi}^2 - V(\phi) + (\gamma - 1)\rho_m, & (7) \end{aligned}$$

$$\ddot{\phi} + 3H\dot{\phi} + V(\phi)_{,\phi} = 0. \quad (8)$$

Question: Is there a way to understand the general evolution of the field equations?
Answer: Yes, we can study the stationary points and their stability.

Universidad Católica del Norte ver más allá
XXX CONGRESO DE MATEMÁTICA CAPRICORNIO COMCA 2022

For $V(\phi) = \frac{\omega^2\phi^2}{2}$, we define

$$\overline{\Omega} = \frac{\sqrt{\dot{\phi}^2 + \omega^2\phi^2}}{\sqrt{6}H}, \quad \overline{\Omega}_m = \frac{\rho_m}{3H^2}, \quad \overline{\Omega}_k = -\frac{k}{a^2H^2}, \tag{9}$$

where

$$\overline{\Omega}^2 + \overline{\Omega}_m + \overline{\Omega}_k = 1. \tag{10}$$

By using the new temporary variable $\tau = \ln a$, the guiding system is obtained:

$$\partial_\tau \overline{\Omega} = \frac{1}{2}\overline{\Omega}\left(3\gamma\overline{\Omega}_m + 3\overline{\Omega}^2 + 2\overline{\Omega}_k - 3\right), \tag{11a}$$

$$\partial_\tau \overline{\Omega}_m = \overline{\Omega}_m\left(3\gamma(\overline{\Omega}_m - 1) + 3\overline{\Omega}^2 + 2\overline{\Omega}_k\right), \tag{11b}$$

$$\partial_\tau \overline{\Omega}_k = \overline{\Omega}_k\left(3\gamma\overline{\Omega}_m + 3\overline{\Omega}^2 + 2\overline{\Omega}_k - 2\right). \tag{11c}$$

Universidad Católica del Norte ver más allá

XXX CONGRESO DE MATEMÁTICA CAPRICORNIO COMCA 2022

Label	$(\overline{\Omega}, \overline{\Omega}_m, \overline{\Omega}_k)$	Eigenvalues	Stability
P_1	$(0,0,0)$	$\{-2, -\frac{3}{2}, -3\gamma\}$	Sink for $0 < \gamma \leq 2$ Nonhyperbolic for $\gamma = 0$
P_2	$(1,0,0)$	$\{3, 1, -3(\gamma-1)\}$	Saddle for $1 < \gamma \leq 2$ Source for $0 \leq \gamma < 1$ Nonhyperbolic for $\gamma = 1$
P_3	$(0,1,0)$	$\{\frac{3(\gamma-1)}{2}, 3\gamma, 3\gamma - 2\}$	Source for $1 < \gamma \leq 2$ Saddle for $0 < \gamma < 2/3, 2/3 < \gamma < 1$ Nonhyperbolic for $\gamma = 0, 2/3, 1$
P_4	$(0,0,1)$	$\{2, -\frac{1}{2}, 2 - 3\gamma\}$	Saddle for $0 \leq \gamma < 2/3, 2/3 < \gamma \leq 2$ Nonhyperbolic for $\gamma = 2/3$

Table: Stability analysis for the equilibrium points of (11).

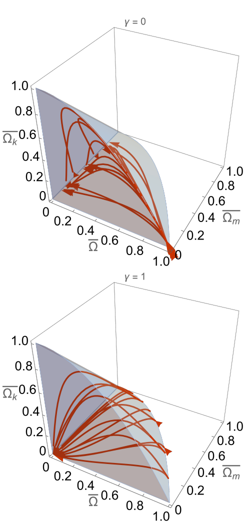

Figure: Phase portrait of system (11) for $\gamma = 0, 2/3, 1, 2$.

Universidad Católica del Norte ver más allá
XXX CONGRESO DE MATEMÁTICA CAPRICORNIO COMCA 2022

12

1. Point P_1 corresponds to a flat FLRW scalar field-dominated solution, that is, a saddle point for $1 < \gamma \leq 2$ (i.e., if the perfect fluid EoS is in the matter domain), or a source for $0 \leq \gamma < 1$ (i.e. if the perfect fluid has a negative pressure).
2. Point P_2 corresponds to the flat FLRW matter-dominated solution, which is unstable to matter perturbations. It is a source for $1 < \gamma \leq 2$ (i.e., if the perfect fluid EoS is in the matter domain) or a saddle if $0 < \gamma < 2/3$ or $2/3 < \gamma < 1$. It corresponds to a transient epoch in cosmological history.
3. Point P_3 is a curvature-dominated solution with positive curvature (Misner solution). The energy density of the scalar field scales as a^{-2} and is a saddle (unstable to curvature perturbations).
4. Finally, point P_4 corresponds to a vacuum Minkowski solution, a sink. The Minkowski solution represents an empty universe. Physically, Minkowski spacetime can be used as a local approximation of spacetime in reasonably small regions and the presence of matter, as long as it does not self-gravitate.

Universidad Católica del Norte
ver más allá

XXX CONGRESO DE MATEMÁTICA CAPRICORNIO
COMCA 2022

- This example would be possible in the context of inflation from an isotropic initial state, and we see that isotropisation is a transient state in the Universe before reaching the Minkowski solution (that is, flat, isotropic, and empty of matter).
- This approach, in which the scalar field oscillates in the minimum before reaching a Minkowski solution, is useful for describing the oscillations of the inflaton around the potential minimum during reheating after inflation.
- This behaviour was described in models like the N-field inflation model as well as in axion-like matter. Fig. 1 shows that the origin is a sink, as indicated in Table 1.

- We define [Clarkson & Barrett, Class. Quant. Grav. 20 (2003) 3855, Clarkson, Phys. Rev. D 76 (2007) 104034]: a unit timelike vector u^a $(u^a u_a = -1)$, the projection tensor on the 3-space $h^a_b = g^a_b + u^a u_b$ and the derivatives:

$$\dot{T}^{a..b}{}_{c..d} = u^e \nabla_e T^{a..b}{}_{c..d} \,, \quad D_e T^{a..b}{}_{c..d} = h^a{}_f h^p{}_c ... h^b{}_g h^q{}_d h^r{}_e \nabla_r T^{f..g}{}_{p..q} \,,$$

- Further, we perform the split of the 3-space by introducing a spacelike vector n^a

$$n_a u^a = 0 \,, \quad n_a n^a = 1 .$$

with a projection tensor on the 2-space (sheet) orthogonal to n^a and u^a

$$N_a{}^b \equiv h_a{}^b - n_a n^b = g_a{}^b + u_a u^b - n_a n^b \,, \;\; N^a{}_a = 2 \,,$$

- Hence we can define two additional derivatives along n^a in the surface orthogonal to u^a, $\hat{T}_{a..b}{}^{c..d} \equiv n^f D_f T_{a..b}{}^{c..d}$, and a projected derivative onto the sheet $\delta_e T_{a..b}{}^{c..d} \equiv N_a{}^f ... N_b{}^g N_i{}^c .. N_j{}^d N_e{}^k D_k T_{f..g}{}^{i..j}$.

Universidad Católica del Norte ver más allá
XXX CONGRESO DE MATEMÁTICA CAPRICORNIO COMCA 2022

15

- The energy-momentum tensor T_{ab} can be decomposed relative to u^a

$$T_{ab} = \rho u_a u_b + p h_{ab} + q_b u_a + q_a u_b + \pi_{ab} \tag{12}$$

ρ: energy density, p: isotropic pressure, $q^a = Q n_a$: energy flux and $\pi_{ab} = \Pi(n_a n_b - \frac{1}{2} N_{ab})$: trace-free anisotropic pressure

- The electric part of the Weyl tensor: $E_{ab} = \mathcal{E}(n_a n_b - \frac{1}{2} N_{ab})$, vorticity free (LRS-II) spacetimes implies magnetic Weyl curvature $H_{ab} = 0$.

- expansion: $\Theta = \nabla_a u^a$, shear: $\Sigma = n^a n^b \nabla_a u_b$, sheet expansion: $\phi = \delta_a n^a$ and the acceleration: $\mathcal{A} = n^a \dot{u}_a$.

Universidad Católica del Norte ver más allá

XXX CONGRESO DE MATEMÁTICA CAPRICORNIO COMCA 2022

Canonical scalar field in static LRS class II spacetimes

$$T_{ab}^{(\psi)} := \nabla_a\psi\nabla_b\psi - \frac{1}{2}g_{ab}\left[(\nabla\psi)^2 + 2V(\psi)\right], \tag{13}$$

we have

$$\rho = \frac{1}{2}\hat{\psi}^2 + V(\psi),$$
$$p = -\frac{1}{6}\hat{\psi}^2 - V(\psi),$$
$$\Pi = \frac{2}{3}\hat{\psi}^2.$$

Universidad Católica del Norte ver más allá

XXX CONGRESO DE MATEMÁTICA CAPRICORNIO COMCA 2022

Static LRS class II spacetimes sourced by a scalar field

$$\hat{\psi} = \Psi, \tag{15a}$$

$$\hat{\phi} = -\frac{1}{2}\phi^2 - \frac{2}{3}\left(\Psi^2 + V(\psi)\right) - \mathcal{E}\,, \tag{15b}$$

$$\hat{\mathcal{E}} = \frac{1}{3}\Psi^2\left(\mathcal{A} - \frac{1}{2}\phi\right) - \frac{3}{2}\phi\mathcal{E}\,, \tag{15c}$$

$$\hat{\mathcal{A}} = -\left(\mathcal{A} + \phi\right)\mathcal{A} - V(\psi) \tag{15d}$$

$$\hat{\Psi} = -\left(\mathcal{A} + \phi\right)\Psi + V'(\psi), \tag{15e}$$

$$\hat{K} = -\phi K\,, \tag{15f}$$

subject to the constraints

$$\mathcal{E} = -\mathcal{A}\phi - \frac{2V(\psi)}{3} + \frac{\Psi^2}{3}, \tag{16a}$$

$$K = \mathcal{A}\phi + V(\psi) - \frac{\Psi^2}{2} + \frac{\phi^2}{4}. \tag{16b}$$

where the Gaussian curvature via the Ricci tensor on the sheet is ${}^2R_{ab} = KN_{ab}$ [Betschart & Clarkson, Class. Quant. Grav. 21 (2004) 5587].

We will use the eq. (16b) to define the dimensionless variables.

$$\begin{aligned} x_1 &= -\frac{\mathcal{E}}{K},\; x_2 = \frac{\phi}{2\sqrt{K}},\; x_3 = \frac{\mathcal{A}}{\sqrt{K}}, \\ y_1 &= \frac{\Psi}{\sqrt{2K}}, y_2 = \frac{V(\psi)}{3K}, \\ \lambda &= -\frac{V_{,\psi}}{V},\; \Gamma = \frac{VV_{,\psi\psi}}{V_{,\psi}^2}, \end{aligned} \tag{17a}$$

Therefore the constraints equations (16a, 16b) become

$$x_2^2 + 2x_2x_3 - y_1^2 + 3y_2 = 1, \tag{18a}$$

$$3x_1 - 6x_2x_3 + 2y_1^2 - 6y_2 = 0. \tag{18b}$$

Universidad Católica del Norte ver más allá

XXX CONGRESO DE MATEMÁTICA CAPRICORNIO COMCA 2022

Reduced dynamical system

$$x_2' = x_2x_3 - y_1^2, \tag{19a}$$
$$x_3' = x_2^2 + x_2x_3 - x_3^2 - y_1^2 - 1, \tag{19b}$$
$$y_1' = \frac{\lambda\left(x_2^2 + 2x_2x_3 - y_1^2 - 1\right)}{\sqrt{2}} - y_1(x_2 + x_3), \tag{19c}$$
$$\lambda' = -\sqrt{2}(\Gamma - 1)\lambda^2 y_1. \tag{19d}$$

where we have introduced the normalized spatial derivative $f' = \frac{\hat{f}}{\sqrt{K}}$. Notice that for positive potential $(y_2 > 0)$, we have from eq.(18a) the condition $x_2(x_2 + 2x_3) - y_1^2 \leq 1$. Therefore for non-negative potentials, the above system defines a flow on the unbounded phase space

$$\left\{(x_2, x_3, y_1, \lambda) : x_2(x_2 + 2x_3) - y_1^2 \leq 1, \lambda \in \mathbb{R}\right\}. \tag{20}$$

Universidad Católica del Norte ver más allá

XXX CONGRESO DE MATEMÁTICA CAPRICORNIO COMCA 2022

We introduce Poincaré variables to study the behaviour of this system at infinity in the phase space:

$$X_2 = \frac{x_2}{\sqrt{1+x_2^2+x_3^2}}, \; X_3 = \frac{x_3}{\sqrt{1+x_2^2+x_3^2}}. \tag{21a}$$

The infinity boundary $x_2^2+x_3^2 \to +\infty$ corresponds to the unitary circle $X_2^2+X_3^2=1$. The evolution equations are

$$\tilde{X}_2 = [1 - X_2(2X_2+X_3)]\left[1-X_2^2-X_3^2\right], \; \tilde{X}_3 = -X_3[2X_2+X_3]\left[1-X_2^2-X_3^2\right], \tag{22}$$

defined on the phase space

$$\left\{(X_2, X_3) : 2X_2^2+2X_2X_3+X_3^2 \geq 1, X_2^2+X_3^2 \leq 1\right\}, \tag{23}$$

where we have rescaled the radial variable through $\tilde{f} \to \sqrt{1-X_2^2-X_3^2} f'$.

Universidad Católica del Norte ver más allá
XXX CONGRESO DE MATEMÁTICA CAPRICORNIO COMCA 2022

21

In the table 2, are presented the critical points at infinity (recall that the circle is a set of critical points) for the Poincaré (global) system (22).

Point	X_2	X_3	Stability	Nature
P_H	0	1	repeller	Horizon
$\bar{P}_H$	0	-1	attractor	Horizon
P_S	$\frac{2}{\sqrt{5}}$	$-\frac{1}{\sqrt{5}}$	repeller	Singularity
$\bar{P}_S$	$-\frac{2}{\sqrt{5}}$	$\frac{1}{\sqrt{5}}$	attractor	Singularity

Table: Critical points at infinity for the Poincaré (global) system (22).

Universidad Católica del Norte ver más allá

XXX CONGRESO DE MATEMÁTICA CAPRICORNIO COMCA 2022

22

We can easily reconstruct the metric using the variables x_2 and x_3. In fact, we have from [A. Ganguly, R. Gannouji, R. Goswami & S. Ray, Class. Quant. Grav. 32 (2015) no.10, 105006], $B = x_2^2$ and $d\ln A/d\ln r = 2x_3/x_2$ where (A, B) are the gravitational potentials defined as

$$ds^2 = -A(r)dt^2 + \frac{dr^2}{B(r)} + r^2\left(d\theta^2 + \sin^2\theta d\phi^2\right) \tag{24}$$

Using the $1+1+2$ decomposition for LRS-II spacetimes, it can be shown that the Misner-Sharp mass takes the following form [G. F. R. Ellis, R. Goswami, A. I. M. Hamid & S. D. Maharaj, Phys. Rev. D 90 (2014) no.8, 084013]

$$\mathcal{M} = \frac{1}{2K^{3/2}}\left(\frac{\rho}{3} - \mathcal{E} - \frac{\Pi}{2}\right) = \frac{1 - x_2^2}{2\sqrt{K}} = \frac{1 - 2X_2^2 - X_3^2}{2\sqrt{K}(1 - X_2^2 - X_3^2)}. \tag{25}$$

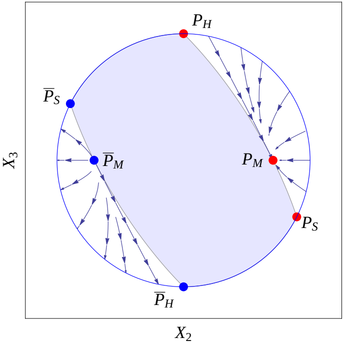

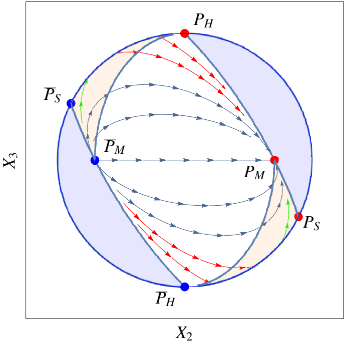

Fig. 1 (a) Global phase space for the system (22). The blue region is forbidden since it leads to the violation of the reality condition $y_1^2 \geq 0$.

Fig. 1 (b) Global phase space for a massless ghost scalar field. The blue region represents the forbidden part of the phase space. A negative Misner-Sharp mass defines the pink region.

1. The critical points $(P_H, \bar{P}_H)$ correspond to horizons because there coordinate is $X_2 = 0$ as shown in [A. Ganguly, R. Gannouji, R. Goswami & S. Ray, Class. Quant. Grav. 32 (2015) no.10, 105006].
2. The points $(P_S, \bar{P}_S)$ correspond to a singularity, in fact, we have from the coordinates $d \ln A / d \ln r = 2x_3/x_2 = 2X_3/X_2 = -1$ which implies $A \propto 1/r$. The same behaviour appears for B. Obviously, at the critical point $B = x_2^2 = \infty$ but after linearization of the system as performed in [A. Ganguly, R. Gannouji, R. Goswami & S. Ray, Class. Quant. Grav. 32 (2015) no.10, 105006] it appears that B diverges as $1/r$.
3. We have only one trajectory and, therefore, one solution connecting the Horizon (P_H) to Minkowski asymptotically (P_M).
   That is the Schwarzschild solution as shown in [A. Ganguly, R. Gannouji, R. Goswami & S. Ray, Class. Quant. Grav. 32 (2015) no.10, 105006]. Any other trajectory starts from a singularity and not from the Horizon and therefore describes a naked singularity.

Universidad Católica del Norte ver más allá
XXX CONGRESO DE MATEMÁTICA CAPRICORNIO COMCA 2022

25

The evolution equations can be written in compact variables as

$$\begin{aligned}
\tilde{X}_2 &= -\frac{\lambda}{\sqrt{2}} X_2 Y_1 \left[2X_2^2 + 2X_2X_3 + X_3^2 - 1\right] + Y_1^2 \left[X_2(2X_2 + X_3) - 1\right] \\
&\quad - X_2 X_3 \left[X_2(3X_2 + X_3) - 2\right], \qquad (26a) \\
\tilde{X}_3 &= -\frac{\lambda}{\sqrt{2}} X_3 Y_1 \left[2X_2^2 + 2X_2X_3 + X_3^2 - 1\right] - 3X_2^2X_3^2 + 2X_2^2 - X_2X_3^3 \\
&\quad + X_3 Y_1^2 (2X_2 + X_3) + X_2X_3 + X_3^2 - 1, \qquad (26b) \\
\tilde{Y}_1 &= \frac{\lambda}{\sqrt{2}} \left[1 - Y_1^2\right] \left[2X_2^2 + 2X_2X_3 + X_3^2 - 1\right] - X_2 Y_1 \left[3X_2X_3 + X_3^2 + 1\right] \\
&\quad + Y_1^3 \left[2X_2 + X_3\right]. \qquad (26c)
\end{aligned}$$

defined on the phase space

$$\left\{(X_2, X_3, Y_1) : 2X_2^2 + 2X_2X_3 + X_3^2 \leq 1, X_2^2 + X_3^2 + Y_1^2 \leq 1\right\}, \qquad (27)$$

where we have rescaled the radial variable through $\tilde{X} \rightarrow \sqrt{1 - X_2^2 - X_3^2 - Y_1^2}\, X'$.

Universidad Católica del Norte ver más allá

XXX CONGRESO DE MATEMÁTICA CAPRICORNIO COMCA 2022

26

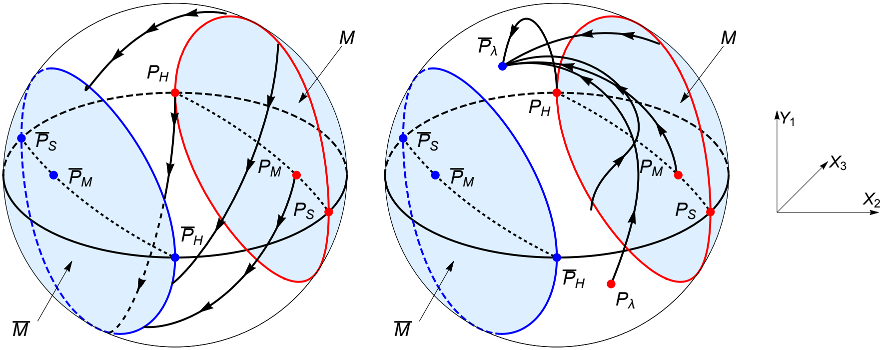

Figure: Phase space of the exponential potential where the blue part represents the forbidden region (phantom scalar field). M and $\bar{M}$ are the phase space boundaries representing two invariant sub-manifolds where most critical points are localised. On the left figure, the phase space is represented with some orbits for $\lambda = 1$ for which all critical points are localised on M and $\bar{M}$, while the right figure represents the orbits for $\lambda = -4$ and therefore P_λ and $\bar{P}_\lambda$ exist.

Universidad Católica del Norte ver más allá
XXX CONGRESO DE MATEMÁTICA CAPRICORNIO COMCA 2022

For the exponential potential, we can analyse two cases:

- The trajectory is over the critical surface (M or $\bar{M}$). This case reduces to a 2D system studied below.
- The trajectory flows from one surface to the other (M to $\bar{M}$).

For the first case, and having in mind that $\bar{M}$ is just the inverse of M, we need to study only the sub-system projected onto the surface M, with parametrization $X_2 = \cos\theta$ and $X_3 = \sin\theta - \cos\theta$, $\theta \in \left[\cos^{-1}\left(\frac{2}{\sqrt{5}}\right), \frac{\pi}{2}\right]$.
The system of the equation on the surface M then becomes

$$\tilde{\theta} = -\left(\frac{\cos\theta - \sin\theta}{2}\right)\left[1 + 2Y_1^2 + \cos(2\theta) - 2\sin(2\theta)\right] \tag{28}$$

$$\tilde{Y}_1 = Y_1\left(\frac{\cos\theta + \sin\theta}{2}\right)\left[1 + 2Y_1^2 + \cos(2\theta) - 2\sin(2\theta)\right], \tag{29}$$

whose orbits are trivially given by

$$Y_1(\theta) = c_1\left[\cos(\theta) - \sin(\theta)\right]. \tag{30}$$

Universidad Católica del Norte ver más allá

XXX CONGRESO DE MATEMÁTICA CAPRICORNIO COMCA 2022

28

Dynamics on the invariant surface M, for the case of exponential potential

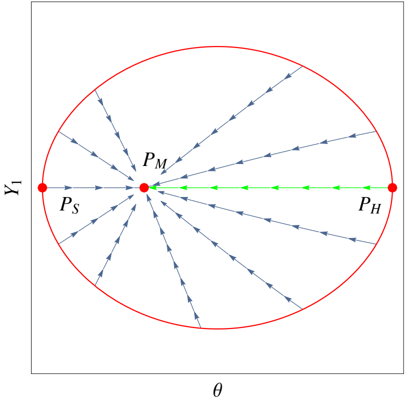

Figure: Phase space of of the system (28)-(29) representing the dynamics on the invariant surface M, for the case of exponential potential.

1. We deduce that we have the same conclusions previously encountered in the massless case.
2. The solution connecting the Horizon (P_H) to an asymptotic flat region (P_M) is unique, and it is the Schwarzschild solution (green curve in Fig. 3). All other solutions exhibit naked singularities.
3. That is consistent with the no-go theorem, which states that for any convex potential ($V_{,\psi\psi} > 0$), the Schwarzschild spacetime is the unique static black hole solution which is asymptotically flat.

After a Poincarè compactification, we found the equations

$$\tilde{X}_2 = -\frac{\lambda}{\sqrt{2}}X_2Y_1\left[2X_2^2+2X_2X_3+X_3^2-1\right]+Y_1^2\left[X_2(2X_2+X_3)-1\right]$$
$$-X_2X_3\left[X_2(3X_2+X_3)-2\right], \tag{31a}$$
$$\tilde{X}_3 = -\frac{\lambda}{\sqrt{2}}X_3Y_1\left[2X_2^2+2X_2X_3+X_3^2-1\right]-3X_2^2X_3^2+2X_2^2-X_2X_3^3$$
$$+X_3Y_1^2(2X_2+X_3)+X_2X_3+X_3^2-1, \tag{31b}$$
$$\tilde{Y}_1 = \frac{\lambda}{\sqrt{2}}\left[1-Y_1^2\right]\left[2X_2^2+2X_2X_3+X_3^2-1\right]-X_2Y_1\left[3X_2X_3+X_3^2+1\right]+Y_1^3[2X_2+X_3], \tag{31c}$$
$$\tilde{\lambda} = -\sqrt{2}Y_1 f(\lambda), \tag{31d}$$

For $V(\psi)>0$, $\left\{(X_2,X_3,Y_1,\lambda): 2X_2^2+2X_2X_3+X_3^2\leq 1, X_2^2+X_3^2+Y_1^2\leq 1, \lambda\in\mathbb{R}\right\}$,
For $V(\psi)<0$, $\left\{(X_2,X_3,Y_1,\lambda): 2X_2^2+2X_2X_3+X_3^2\geq 1, X_2^2+X_3^2+Y_1^2\leq 1, \lambda\in\mathbb{R}\right\}$.

Universidad Católica del Norte ver más allá
XXX CONGRESO DE MATEMÁTICA CAPRICORNIO COMCA 2022

Fixed point for an Arbitrary Potential

Point	X_2	X_3	Y_1	λ	Existence	Stability	Nature
P_H	0	1	0	λ_c	$\lambda_c \in \mathbb{R}$	unstable	Horizon
$\bar{P}_H$	0	-1	0	λ_c	$\lambda_c \in \mathbb{R}$	stable	Horizon
P_S	$\frac{2}{\sqrt{5}}$	$-\frac{1}{\sqrt{5}}$	0	λ_c	$\lambda_c \in \mathbb{R}$	unstable	Singularity
$\bar{P}_S$	$-\frac{2}{\sqrt{5}}$	$\frac{1}{\sqrt{5}}$	0	λ_c	$\lambda_c \in \mathbb{R}$	stable	Singularity
P_M	$\frac{1}{\sqrt{2}}$	0	0	λ_c	$\lambda_c \in \mathbb{R}$	saddle	Minkowski
$\bar{P}_M$	$-\frac{1}{\sqrt{2}}$	0	0	λ_c	$\lambda_c \in \mathbb{R}$	saddle	Minkowski
P_{AdS}	$\frac{1}{\sqrt{2}}$	$\frac{1}{\sqrt{2}}$	0	0	$V(\psi) < 0$	stable for $f(0) > 0$	Anti-de Sitter
$\bar{P}_{AdS}$	$-\frac{1}{\sqrt{2}}$	$-\frac{1}{\sqrt{2}}$	0	0	$V(\psi) < 0$	unstable for $f(0) > 0$	Anti-de Sitter
$P(\lambda^\star)$	$\sqrt{\frac{2}{(\lambda^\star)^2+4}}$	$\sqrt{\frac{2}{(\lambda^\star)^2+4}}$	$\frac{\lambda^\star}{\sqrt{(\lambda^\star)^2+4}}$	$\lambda^\star$	$f(\lambda^\star) = 0,$ $(\lambda^\star)^2 \geq 6$	unstable for $f'(\lambda^\star) < 0, \lambda^\star > \sqrt{6},$ or $f'(\lambda^\star) > 0, \lambda^\star < -\sqrt{6}$ saddle otherwise	$A \propto r^2,$ $B \propto r^{2-(\lambda^\star)^2}$ singularity
$\bar{P}(\lambda^\star)$	$-\sqrt{\frac{2}{(\lambda^\star)^2+4}}$	$-\sqrt{\frac{2}{(\lambda^\star)^2+4}}$	$-\frac{\lambda^\star}{\sqrt{(\lambda^\star)^2+4}}$	$\lambda^\star$	$f(\lambda^\star) = 0,$ $(\lambda^\star)^2 \geq 6$	stable for $f'(\lambda^\star) < 0, \lambda^\star > \sqrt{6},$ or $f'(\lambda^\star) > 0, \lambda^\star < -\sqrt{6}$ saddle otherwise	$A \propto r^2,$ $B \propto r^{2-(\lambda^\star)^2}$ singularity

Universidad Católica del Norte ver más allá

XXX CONGRESO DE MATEMÁTICA CAPRICORNIO COMCA 2022

Point	X_2	X_3	Y_1	λ	Existence	Stability	Nature
$\mathcal{C}(\lambda^\star)$	$\cos\theta$	$\sin\theta-\cos\theta$	$\sqrt{1-X_2^2-X_3^2}$	$\lambda^\star$	$f(\lambda^\star)=0$	M is unstable for $f'(\lambda^\star)<0$, $\lambda^\star<\frac{2\cos(\theta)+2\sin(\theta)}{\sqrt{-1-\cos(2\theta)+2\sin(2\theta)}}$	singularity
	$\cos\theta$	$\sin\theta-\cos\theta$	$-\sqrt{1-X_2^2-X_3^2}$	$\lambda^\star$	$f(\lambda^\star)=0$	M is unstable for $f'(\lambda^\star)>0$, $\lambda^\star>-\frac{2\cos(\theta)+2\sin(\theta)}{\sqrt{-1-\cos(2\theta)+2\sin(2\theta)}}$ saddle otherwise	singularity
$\bar{\mathcal{C}}(\lambda^\star)$	$\cos\theta$	$-\sin\theta-\cos\theta$	$\sqrt{1-X_2^2-X_3^2}$	$\lambda^\star$	$f(\lambda^\star)=0$	M is stable for $f'(\lambda^\star)>0$, $\lambda^\star>\frac{2\cos(\theta)-2\sin(\theta)}{\sqrt{-1-\cos(2\theta)+2\sin(2\theta)}}$	singularity
	$\cos\theta$	$-\sin\theta-\cos\theta$	$-\sqrt{1-X_2^2-X_3^2}$	$\lambda^\star$	$f(\lambda^\star)=0$	M is stable for $f'(\lambda^\star)<0$, $\lambda^\star<-\frac{2\cos(\theta)-2\sin(\theta)}{\sqrt{-1-\cos(2\theta)+2\sin(2\theta)}}$ saddle otherwise	singularity

Universidad Católica del Norte ver más allá

XXX CONGRESO DE MATEMÁTICA CAPRICORNIO COMCA 2022

Martinez-Troncoso-Zanelli (MTZ) black hole

The relations $V(\psi) < 0$ and $f(0) > 0$ are very useful to check if a model has solutions which are asymptotically AdS (AAdS). For example, the Martinez-Troncoso-Zanelli (MTZ) black hole is AAdS [C. Martinez, R. Troncoso and J. Zanelli, Phys. Rev. D **70** (2004) 084035 [hep-th/0406111]]. For this model, the potential is defined as

$$V(\psi) = \Lambda\left[1 + 2\sinh\left(\frac{\psi}{\sqrt{6}}\right)\right], \ \Lambda < 0 \tag{32}$$

It is easy to check that for this potential $f(\lambda) = 2/3 - \lambda^2$ and therefore $f(0) > 0$, which implies that an AAdS solution exists, which is the MTZ black hole.

- We reformulated some of the important results about black holes in the presence of a scalar field.
- In the first case, where the potential is zero, we recovered all results for the black hole and the conditions for the existence of a wormhole. We found that except the Schwarzschild solution, all other solutions are naked singularities.
- The same analysis has been extended to the exponential potential. We found that black hole solution asymptotically flat is unique, and it is the Schwarzschild solution; all other solutions are naked singularities. We also found other solutions which connect the two regions of the phase space through $x_2 = 0$ as a wormhole but by violating the flare-out condition, implying a maximum radius instead of a throat. Nevertheless, all these solutions are naked because they connect two singularities.
- Finally, a generic result has been derived. For any potential which is not asymptotically zero, the unique black hole solution is Schwarzschild.

MUCHAS GRACIAS

Universidad Católica del Norte
ver más allá

XXX CONGRESO DE MATEMÁTICA CAPRICORNIO
COMCA 2022

1. Periodic averaging
   (a) The Van der Pol equation
2. LRS Bianchi III Einstein-Klein-Gordon system
   (a) The system in the quasi-standard form
   (b) Averaging conjecture
3. Generalized harmonic potentials
   (a) Averaging generalized scalar-field cosmologies with matter
   (b) Late-time behaviour

The theory of averaging studies initial value problems of the general form

$$\dot{\mathbf{x}} = \mathbf{f}(\mathbf{x}, t, \epsilon), \quad \mathbf{x}(0) = \mathbf{a},$$

with $\mathbf{x}, \mathbf{f}(\mathbf{x}, t, \epsilon) \in \mathbb{R}^n$, where ϵ plays the role of a, usually small, perturbation parameter. One is typically looking at problems of the standard form

$$\dot{\mathbf{x}} = \epsilon\, \mathbf{f}^1(\mathbf{x}, t) + \epsilon^2\, \mathbf{f}^{[2]}(\mathbf{x}, t, \epsilon), \quad \mathbf{x}(0) = \mathbf{a}, \tag{33}$$

with $\mathbf{f}^1$ and $\mathbf{f}^{[2]}$ T-periodic in t. The exponents correspond to the respective perturbation order, and the square bracket marks the remainder of the series; cf [Sanders, Verhulst & Murdock, 2010, p 13, Notation 1.5.2].
To first order, the theory is then concerned with the Question to what degree solutions of (33) can be approximated by the solutions of an associated *averaged system*

$$\dot{\mathbf{z}} = \epsilon\, \bar{\mathbf{f}}^1(\mathbf{z}), \quad \mathbf{z}(0) = \mathbf{a}, \; \bar{\mathbf{f}}^1(\mathbf{z}) = \frac{1}{T}\int_0^T \mathbf{f}^1(\mathbf{z}, s)\, \mathrm{d}s. \tag{34}$$

Take the following two definitions from [Sanders, Verhulst & Murdock, 2010, p 31] and [Sanders, Verhulst & Murdock, 2010, Def 4.2.4] respectively.

Definition

$D \subset \mathbb{R}^n$ is a connected, bounded open set (with compact closure) containing the initial value $\mathbf{a}$, and constants $L > 0, \epsilon_0 > 0$, such that the solutions $\mathbf{x}(t,\epsilon)$ and $\mathbf{z}(t,\epsilon)$ with $0 \leq \epsilon \leq \epsilon_0$ remain in D for $0 \leq t \leq L/\epsilon$.

See also the comments on [Sanders, Verhulst & Murdock, 2010, p 31] how such a triple (D, ϵ_0, L) can be chosen.

Definition

Consider the vector field $\mathbf{f}(\mathbf{x},t)$ with $\mathbf{f} : \mathbb{R}^n \times \mathbb{R} \to \mathbb{R}^n$. Let $\mathbf{f}$ be Lipschitz continuous in $\mathbf{x}$ on $D \subset \mathbb{R}^n, t \geq 0$. Let further $\mathbf{f}$ be continuous in t and $\mathbf{x}$ on $\mathbb{R}^+ \times D$. If the average

$$\bar{\mathbf{f}}(\mathbf{x}) = \lim_{T\to\infty} \frac{1}{T} \int_0^T \mathbf{f}(\mathbf{x},s)\mathrm{d}s$$

*exists and the limit is uniform in $\mathbf{x}$ on compact subsets of D, then $\mathbf{f}$ is called a **KBM-vector field** (Krylov, Bogoliubov and Mitropolsky).*
(If the vector field $\mathbf{f}(\mathbf{x},t)$ contains parameters, we assume that the parameters and the initial conditions are independent of ϵ and that the limit is uniform in the parameters.)

The following theorem gives the basic result:

Lemma ([Sanders, Verhulst & Murdock, 2010, p 31, Thm 2.8.1])

Let $\mathbf{f}^1$ *be Lipschitz continuous, let* $\mathbf{f}^{[2]}$ *be continuous, and let* ϵ_0, D, L *be as in* DEFINITION 3.1. *Then there exists a constant* $c > 0$ *such that*

$$||\mathbf{x}(t,\epsilon) - \mathbf{z}(t,\epsilon)|| < c\epsilon$$

for $0 \leq \epsilon \leq \epsilon_0$ *and* $0 \leq t \leq L/\epsilon$, *and where* $||\,.\,||$ *denotes the norm* $||\mathbf{u}|| := \sum_{i=1}^{n} |u_i|$ *for* $\mathbf{u} \in \mathbb{R}^n$.

In other words, the error one makes by approximating the full system (33) by the averaged system (34) will be of order ϵ on timescales of order ϵ^{-1}. When the solutions of the full or averaged asymptotically stable critical point attract system, the domain of approximation might be extendable to all times;
cf [Sanders, Verhulst & Murdock, 2010, Chap 5].

For instance:

Lemma (Eckhaus/Sanchez-Palencia [Sanders, Verhulst & Murdock, 2010, p 101, Thm 5.5.1])

Consider the initial value problem

$$\dot{\mathbf{x}} = \epsilon\, \mathbf{f}^1(\mathbf{x}, t), \quad \mathbf{x}(0) = \mathbf{a},$$

with $\mathbf{a}, \mathbf{x} \in D \subset \mathbb{R}^n$ *and* $\mathbf{f}^1$ *T-periodic in t. Suppose* $\mathbf{f}^1$ *is a KBM-vector field* (Definition 3.2) *producing the averaged equation*

$$\dot{\mathbf{z}} = \epsilon\, \overline{\mathbf{f}}^1(\mathbf{z}), \quad \mathbf{z}(0) = \mathbf{a},$$

where $\mathbf{z} = 0$ *is an asymptotically stable critical point in the linear approximation,* $\overline{\mathbf{f}}^1$ *is continuously differentiable for* $\mathbf{z}$ *in D and has a domain of attraction* $D^o \subset D$*. Then for any compact* $K \subset D^o$ *and all* $\mathbf{a} \in K$

$$\mathbf{x}(t) - \mathbf{z}(t) = \mathcal{O}(\epsilon), \quad 0 \leq t < \infty.$$

Universidad Católica del Norte ver más allá

XXX CONGRESO DE MATEMÁTICA CAPRICORNIO COMCA 2022

41

Given the class of Van der Pol equations

$$\ddot{\phi} + \phi = \epsilon\, g(\phi, \dot{\phi}) \tag{35}$$

with g sufficiently smooth. (35) describes a harmonic oscillator with generally nonlinear feedback and damping. An amplitude-phase (variation of constants) transformation yields a system in standard form (33)

$$\begin{aligned} \phi &= r\sin(t-\varphi) \\ \dot{\phi} &= r\cos(t-\varphi) \end{aligned} \quad \Longrightarrow \quad \begin{bmatrix} \dot{r} \\ \dot{\varphi} \end{bmatrix} = \epsilon \begin{bmatrix} \cos(t-\varphi)\, g(\phi, \dot{\phi}) \\ \frac{1}{r}\sin(t-\varphi)\, g(\phi, \dot{\phi}) \end{bmatrix} \tag{36}$$

where the arguments of g are understood to be substituted by the transformation. Consequently, the averaged system (34) is given by

$$\begin{bmatrix} \dot{\overline{r}} \\ \dot{\overline{\varphi}} \end{bmatrix} = \epsilon\, \overline{\mathbf{f}}^1(\overline{r}) = \epsilon \begin{bmatrix} \overline{f}^1_r(\overline{r}) \\ \overline{f}^1_\varphi(\overline{r}) \end{bmatrix} \tag{37}$$

with $\overline{f}^1_r(\overline{r}) = \frac{1}{2\pi}\int_0^{2\pi} \cos(s-\overline{\varphi})\, g\left(\overline{r}\sin(s-\overline{\varphi}), \overline{r}\cos(s-\overline{\varphi})\right) \mathrm{d}s$. Furthermore, $\overline{f}^1_\varphi(r)$ defined analogously. Note that $\overline{\mathbf{f}}^1$ is independent of $\overline{\varphi}$.

Specialising now to the specific Van der Pol equation with $g(\phi, \dot{\phi}) = (1 - \phi^2)\dot{\phi}$ as an illustrative example we obtain the averaged system

$$\begin{bmatrix} \dot{\bar{r}} \\ \dot{\bar{\varphi}} \end{bmatrix} = \begin{bmatrix} \frac{1}{2}\epsilon\bar{r}(1 - \frac{1}{4}\bar{r}^2) \\ 0 \end{bmatrix}. \tag{38}$$

By LEMMA 1 we know that the error between $[r, \varphi]^{\mathrm{T}}$ and $[\bar{r}, \bar{\varphi}]^{\mathrm{T}}$ will be of order ϵ on timescales of order ϵ^{-1}. Since $\bar{\mathbf{f}}^1$ is independent of $\bar{\varphi}$ we restrict to the decoupled equation $\dot{\bar{r}}$, which has the two equilibrium points $\bar{r} = 0$ and $\bar{r} = 2$. The equilibrium point $\bar{r} = 2$ is stable, and we can apply LEMMA 2 to extend the validity of the $\mathcal{O}(\epsilon)$ error estimate to all times into the future. (Similarly, by defining a negative time variable, we could apply the theorem to the past attraction to the unstable critical point at the origin.)

Universidad Católica del Norte ver más allá

XXX CONGRESO DE MATEMÁTICA CAPRICORNIO COMCA 2022

An LRS Bianchi III metric can be written in the form [Fajman, Heißel & Maliborski, 2020]

$$\mathbf{g} = -\mathrm{d}t^2 + a(t)^2\,\mathrm{d}r^2 + b(t)^2\,\mathbf{g}_{H^2} \tag{39}$$

where $\mathbf{g}_{H^2} = d\vartheta^2 + \sinh^2(\vartheta)d\zeta^2$ denotes the 2-metric of negative constant curvature on hyperbolic 2-space.
The resulting dynamical systems formulation of the Einstein equations for the metric (39) and an energy-momentum tensor of the form $[T^a{}_b] = \mathrm{diag}(-\rho, p, p, p)$. For a Klein-Gordon field of mass 1 and the metric (39) we have

$$\rho = \frac{1}{2}(\dot{\phi}^2 + \phi^2) \quad \text{and} \quad p = \frac{1}{2}(\dot{\phi}^2 - \phi^2) \tag{40}$$

where the field ϕ is subject to the Klein-Gordon equation $\Box_{\mathbf{g}}\phi = \phi$. Note that the Einstein equations force ϕ to be independent of the spatial coordinates due to spatial homogeneity. Some of the equations are decoupled.

For this presentation, it suffices to restrict to the reduced coupled part of the LRS Bianchi III Einstein-Klein-Gordon system, which is given by [Fajman, Heißel & Maliborski, 2020]

$$\dot{H} = H^2[-(1+q)] \tag{41}$$

$$\dot{\Sigma}_+ = H[-(2-q)\Sigma_+ + 1 - \Sigma_+^2 - \Omega] \tag{42}$$

$$\ddot{\phi} + \phi = H[-3\dot{\phi}], \tag{43}$$

with the *deceleration parameter*

$$q = 2\Sigma_+^2 + \frac{1}{6H^2}\left(2\dot{\phi}^2 - \phi^2\right). \tag{44}$$

$H := (\frac{\dot{a}}{a} + 2\frac{\dot{b}}{b})/3$ denotes the *Hubble scalar*, i.e., a measure of the overall isotropic rate of spatial expansion. The corresponding evolution equation (41) is also referred to as the *Raychaudhuri equation*.
$H\Sigma_+ := (\frac{\dot{a}}{a} - \frac{\dot{b}}{b})/3$ denotes the only independent component of the *shear tensor*, i.e., a measure of anisotropy in the rate of spatial expansion.
Finally, $\Omega := \rho/(3H^2)$ defines a re-scaled energy density which is non-negative by definition. Since we are interested in non-vacuum solutions, we consider Ω to be positive.

The variables are subject to the *Hamiltonian constraint*

$$1 - \Sigma_+^2 - \Omega > 0. \tag{45}$$

Consequently, Σ_+ and Ω are bounded and take values in the range $(-1, 1)$ and $(0, 1)$ respectively. The Klein-Gordon field ϕ is unbounded, and so is H a priori. However, one will restrict the interest to the case of an (initially) expanding universe, i.e. to $H > 0$.

The Klein-Gordon equation (43) has the form of a Van der Pol equation (35) with $g(\phi, \dot{\phi}) = -3\dot{\phi}$ and where $H(t)$ plays the role of ϵ. The system (41)–(43) therefore describes a harmonic oscillator with nonlinear damping, where the time dependence of the latter is governed by the coupling of the Einstein equations with the Klein-Gordon equation via H.

Universidad Católica del Norte ver más allá

XXX CONGRESO DE MATEMÁTICA CAPRICORNIO COMCA 2022

The system in quasi-standard form

Following Subsection 1 an amplitude-phase transformation (36) to formulate the Klein-Gordon equation (43) as two first order equations is applied. Furthermore, a transform is used,

$$r \mapsto \Omega = r^2/(6H^2) \quad \Longrightarrow \quad q = 2\Sigma_+^2 + \Omega\big(3\cos^2(t-\varphi) - 1\big). \tag{46}$$

The result is the system (41), (42) together with the first order Klein-Gordon equations

$$\dot{\Omega} = H\big[2\Omega\big(1 + q - 3\cos^2(t-\varphi)\big)\big] \tag{47}$$

$$\dot{\varphi} = H[-3\sin(t-\varphi)\cos(t-\varphi)]. \tag{48}$$

Moreover, where now q is understood to be expressed by (46). Setting $\mathbf{x} = [\Sigma_+, \Omega, \varphi]^{\mathrm{T}}$ this system has the form

$$\begin{bmatrix} \dot{H} \\ \dot{\mathbf{x}} \end{bmatrix} = H\,\mathbf{F}^1(\mathbf{x},t) + H^2\,\mathbf{F}^{[2]}(\mathbf{x},t) = H\begin{bmatrix} 0 \\ \mathbf{f}^1(\mathbf{x},t) \end{bmatrix} + H^2\begin{bmatrix} f^{[2]}(\mathbf{x},t) \\ \mathbf{0} \end{bmatrix} \tag{49}$$

where $\mathbf{f}^1(\mathbf{x},t)$ is given by the square brackets in (42), (47) and (48), and $f^{[2]}(\mathbf{x},t)$ by the square bracket in (41). Note that $\mathbf{f}^1, f^{[2]}$ are independent of H. One can see that (49) resembles the standard form (33) with $H(t)$ playing the role of the perturbation parameter ϵ.

47

Because (49) has only quasi-standard form and not standard form; one cannot directly apply lemmas 1 or 2 to obtain rigorous error estimates. However, the following conjecture is formulated.

Conjecture

Consider some arbitrary non-vacuum ($\Omega > 0$) initial value satisfying the Hamiltonian constraint (45) and $H > 0$. Let $[H(t), \mathbf{x}(t)]^{\mathrm{T}}$ denote the respective solution to (49) and let $\mathbf{z}(t)$ denote the solution to the corresponding averaged equation $\dot{\mathbf{z}} = H(t)\, \bar{\mathbf{f}}^{1}(\mathbf{z})$, with $\bar{\mathbf{f}}^{1}$ as in (34). Let $\mathbf{X}(t), \mathbf{Z}(t)$ denote the 2-vectors containing the Σ_+ and Ω components of the corresponding 3-vectors $\mathbf{x}(t), \mathbf{z}(t)$. Then there exists a t_* such that

$$\mathbf{X}(t) - \mathbf{Z}(t) = \mathcal{O}\big(H(t)\big) \quad \forall\, t > t_*. \tag{50}$$

Under the premise that it holds, one then derives the future asymptotic of Bianchi III Einstein-Klein-Gordon cosmologies.
In [Fajman, Heißel & Jang, 2021] the long-term behaviour of solutions of a general class of systems in the standard form (49) was studied; where $H > 0$ is strictly decreasing in t and $\lim_{t\to\infty} H(t) = 0$.

Let the norm $\|\cdot\|$ denotes the standard discrete ℓ^1- norm $\|\mathbf{u}\| := \sum_i^n |u_i|$ for $\mathbf{u} \in \mathbb{R}^n$. Let also $L^\infty_{\mathbf{x},t}$ denotes the standard L^∞ space in both t and $\mathbf{x}$ variables with norm defined as $\|\mathbf{f}\|_{L^\infty_{\mathbf{x},t}} := \sup_{\mathbf{x},t} |\mathbf{f}(\mathbf{x},t)|$.

Theorem (Theorem 3.1 of [Fajman, Heißel & Jang, 2021])

Suppose $H(t) > 0$ is strictly decreasing in t and $\lim_{t\to\infty} H(t) = 0$. Fix any $\epsilon > 0$ with $\epsilon < H(0)$ and define $t_* > 0$ such that $\epsilon = H(t_*)$. Suppose that $\|\mathbf{f}^1\|_{L^\infty_{\mathbf{x},t}}, \quad \|f^{[2]}\|_{L^\infty_{\mathbf{x},t}} < \infty$ and that $\mathbf{f}^1(\mathbf{x},t)$ is Lipschitz continuous and $f^{[2]}$ is continuous with respect to x for all $t \geq t_*$. Also, assume that $\mathbf{f}^1$ and $f^{[2]}$ are T-periodic for some $T > 0$. Then for all $t > t_*$ with $t = t_* + \mathcal{O}\left(H(t_*)^{-\delta}\right)$ for any given $\delta \in (0,1)$ we have

$$\mathbf{x}(t) - \mathbf{z}(t) = \mathcal{O}\left(H(t_*)^{\min\{1,2-2\delta\}}\right),$$

where $\mathbf{x}$ is the solution of system (49) with initial condition $\mathbf{x}(0) = \mathbf{x}_0$ and $\mathbf{z}(t)$ is the solution of the time-averaged system $\dot{\mathbf{z}} = H(t_*)\bar{\mathbf{f}}^1(\mathbf{z}), \quad \text{for} \quad t > t_*$, with initial condition $\mathbf{z}(t_*) = \mathbf{x}(t_*)$ where the time-averaged vector $\bar{\mathbf{f}}^1$ is defined as

$$\bar{\mathbf{f}}^1(\mathbf{z}) = \frac{1}{T}\int_{t_*}^{t_*+T} \mathbf{f}^1(\mathbf{z},s)ds.$$

We study a scalar-filed cosmology with potential

$$V(\phi) = \mu^2\phi^2 + \underbrace{f^2\left(\omega^2 - 2\mu^2\right)}_{b\mu^3+2f\mu^2-f\omega^2=0, \quad \omega^2-2\mu^2>0} \left(1 - \cos\left(\frac{\phi}{f}\right)\right). \tag{51}$$

1. V is a real-valued smooth function $V \in C^\infty(\mathbb{R})$ with $\lim_{\phi\to\pm\infty} V(\phi) = +\infty$.
2. V is an even function $V(\phi) = V(-\phi)$.
3. $V(\phi)$ has always a local minimum at $\phi = 0$; $V(0) = 0, V'(0) = 0, V''(0) = \omega^2 > 0$.
4. There is a finite number of values $\phi_c \neq 0$ satisfying $2\mu^2\phi_c + f\left(\omega^2 - 2\mu^2\right)\sin\left(\frac{\phi_c}{f}\right) = 0$ which are local maximums or local minimums depending on whether $V''(\phi_c) < 0$ or $V''(\phi_c) > 0$. For $|\phi_c| > \frac{f(\omega^2-2\mu^2)}{2\mu^2} = \phi_*$ this set is empty.
5. There exist $V_{\max} = \max_{\phi\in[-\phi_*,\phi_*]} V(\phi)$ and $V_{\min} = \min_{\phi\in[-\phi_*,\phi_*]} V(\phi) = 0$.

The asymptotic features of potential (51) are the following. Near global minimum $\phi = 0$, we have $V(\phi) \sim \frac{\omega^2\phi^2}{2} + \mathcal{O}\left(\phi^3\right)$, as $\phi \to 0$. That is, ω^2 can be related to the mass of the scalar field near its global minimum. As $\phi \to \pm\infty$ cosine-correction is bounded, then, $V(\phi) \sim \mu^2\phi^2 + \mathcal{O}(1)$, as $\phi \to \pm\infty$. That makes it suitable to describe oscillatory behaviour in cosmology.

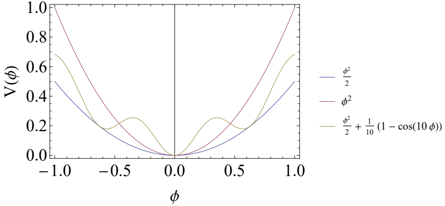

(a) $V(\phi)$ defined by (51) for $\mu = \frac{\sqrt{2}}{2}$, $\omega = \sqrt{\left|\frac{f-1}{f}\right|}i$, $f = \frac{1}{10}$.

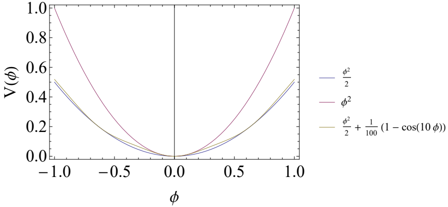

(b) $V(\phi)$ defined by (51) for $\mu = \frac{\sqrt{2}}{2}$, $\omega = \sqrt{2}$, $f = \frac{1}{10}$

Figure: Generalised harmonic potentials. Comparison with ϕ-squared potentials.

Here we study systems which are not in the standard form (49) but can be expressed as a series with the centre in $H = 0$ according to the equation

$$\begin{pmatrix} \dot{H} \\ \dot{\mathbf{x}} \end{pmatrix} = \begin{pmatrix} 0 \\ \mathbf{f}^0(\mathbf{x}, t) \end{pmatrix} + H \begin{pmatrix} 0 \\ \mathbf{f}^1(\mathbf{x}, t) \end{pmatrix} + H^2 \begin{pmatrix} f^{[2]}(\mathbf{x}, t) \\ \mathbf{0} \end{pmatrix} + \mathcal{O}(H^3), \tag{52}$$

depending on a parameter ω which is a free frequency that can be tuned to make $\mathbf{f}^0(\mathbf{x}, t) = \mathbf{0}$. Therefore, systems can be expressed in the standard form (49).
We define the time averaging

$$\bar{\mathbf{f}}(\cdot) := \frac{1}{L} \int_0^L \mathbf{f}(\cdot, t) dt, \quad L = \frac{2\pi}{\omega}. \tag{53}$$

LRS Bianchi III

Defining $\mathbf{x} = (\Omega, \Sigma, \Omega_k, \Phi)^T$, the system can be symbolically written as a Taylor series of the form (52). Notice that the term

$$\mathbf{f}^0(t, \mathbf{x}) = \begin{pmatrix} \frac{\Omega\left(f\omega^2 - \mu^2(b\mu + 2f)\right)\sin(2t\omega - 2\Phi)}{2f\omega} \\ 0 \\ \frac{\left(-b\mu^3 - 2f\mu^2 + f\omega^2\right)\sin^2(t\omega - \Phi)}{f\omega} \\ 0 \end{pmatrix} \tag{54}$$

in expression (52) is eliminated imposing the condition $b\mu^3 + 2f\mu^2 - f\omega^2 = 0$, which defines an angular frequency $\omega \in \mathbb{R}$. Then, order zero terms in the series expansion around $H = 0$ are eliminated assuming $\omega^2 > 2\mu^2$ and setting $f = \frac{b\mu^3}{\omega^2 - 2\mu^2}$, which is equivalent to tune ω.

Universidad Católica del Norte ver más allá

XXX CONGRESO DE MATEMÁTICA CAPRICORNIO COMCA 2022

Hence, we obtain:

$$\dot{\mathbf{x}} = H\mathbf{f}(t,\mathbf{x}) + \mathcal{O}(H^2), \tag{55}$$

$$\dot{H} = -\frac{3}{2}H^2\left(\gamma(1-\Sigma^2-\Omega_k-\Omega^2) + 2\Sigma^2 + \frac{2}{3}\Omega_k + 2\Omega^2\cos^2(t\omega-\Phi)\right) + \mathcal{O}(H^3), \tag{56}$$

where

$$\mathbf{f}(t,\mathbf{x}) = \begin{pmatrix} \frac{1}{2}\Omega\Big(-3(\gamma-2)\Sigma^2 + (2-3\gamma)\Omega_k + 3\left(\Omega^2-1\right)\left(-\gamma+2\cos^2(t\omega-\Phi)\right)\Big) \\ \frac{1}{2}\left(\Omega_k((2-3\gamma)\Sigma+2) + 3\Sigma\Big(-(\gamma-2)\Sigma^2+\gamma+\Omega^2(-\gamma+2\cos^2(t\omega-\Phi))-2\Big)\right) \\ \Omega_k\Big(-3\gamma\left(\Sigma^2+\Omega^2+\Omega_k-1\right) + 6\Sigma^2 - 2\Sigma + 6\Omega^2\cos^2(t\omega-\Phi) + 2\Omega_k - 2\Big) \\ -\frac{3}{2}\sin(2t\omega-2\Phi) \end{pmatrix}. \tag{57}$$

Replacing $\dot{\mathbf{x}} = H\mathbf{f}(t,\mathbf{x})$ where $\mathbf{f}(t,\mathbf{x})$ is defined by (57) with $\dot{\mathbf{y}} = H\bar{\mathbf{f}}(\mathbf{y})$, $\mathbf{y} = \left(\overline{\Omega}, \overline{\Sigma}, \overline{\Omega}_k, \overline{\Phi}\right)^T$ and $\bar{\mathbf{f}}(\mathbf{y})$ given by time-averaging (53) we obtain:

$$\dot{\overline{\Omega}} = \frac{1}{2}H\overline{\Omega}\Big(-3\gamma\left(\overline{\Sigma}^2 + \overline{\Omega}^2 + \overline{\Omega}_k - 1\right) + 6\overline{\Sigma}^2 + 3\overline{\Omega}^2 + 2\overline{\Omega}_k - 3\Big), \tag{58}$$

$$\dot{\overline{\Sigma}} = \frac{1}{2}H\left(\overline{\Sigma}\Big(-3\gamma\left(\overline{\Sigma}^2 + \overline{\Omega}^2 + \overline{\Omega}_k - 1\right) + 6\overline{\Sigma}^2 + 3\overline{\Omega}^2 + 2\overline{\Omega}_k - 6\Big) + 2\overline{\Omega}_k\right), \tag{59}$$

$$\dot{\overline{\Omega}}_k = -H\overline{\Omega}_k\Big(3\gamma\left(\overline{\Sigma}^2 + \overline{\Omega}^2 + \overline{\Omega}_k - 1\right) - 6\overline{\Sigma}^2 + 2\overline{\Sigma} - 3\overline{\Omega}^2 - 2\overline{\Omega}_k + 2\Big), \tag{60}$$

$$\dot{\overline{\Phi}} = 0, \tag{61}$$

$$\dot{H} = -\frac{1}{2}H^2\Big(3\gamma\left(1 - \overline{\Sigma}^2 - \overline{\Omega}^2 - \overline{\Omega}_k\right) + 6\overline{\Sigma}^2 + 3\overline{\Omega}^2 + 2\overline{\Omega}_k\Big). \tag{62}$$

Universidad Católica del Norte
ver más allá

XXX CONGRESO DE MATEMÁTICA CAPRICORNIO
COMCA 2022

Let us define the transformation

$$\mathbf{x}_0 := (\Omega_0, \Sigma_0, \Omega_{k0}, \Phi_0)^T \mapsto \mathbf{x} := (\Omega, \Sigma, \Omega, \Phi)^T$$

$$\mathbf{x} = \psi(\mathbf{x}_0) := \mathbf{x}_0 + H\mathbf{g}(H, \mathbf{x}_0, t), \quad \mathbf{g}(H, \mathbf{x}_0, t) = \begin{pmatrix} g_1(H, \Omega_0, \Sigma_0, \Omega_{k0}, \Phi_0, t) \\ g_2(H, \Omega_0, \Sigma_0, \Omega_{k0}, \Phi_0, t) \\ g_3(H, \Omega_0, \Sigma_0, \Omega_{k0}, \Phi_0, t) \\ g_4(H, \Omega_0, \Sigma_0, \Omega_{k0}, \Phi_0, t) \end{pmatrix}. \tag{63}$$

Theorem

Let $\overline{\Omega}, \overline{\Sigma}, \overline{\Omega}_k, \overline{\Phi}$ and H be defined functions that satisfy averaged equations (58), (59), (60), (61), (62). Then, there exist continuously differentiable functions g_1, g_2, g_3 and g_4, such that Ω, Σ, Ω_k and Φ are locally given by (63), where $\Omega_0, \Sigma_0, \Omega_{k0}, \Phi_0$ are order zero approximations of them as $H \to 0$. Then, functions $\Omega_0, \Sigma_0, \Omega_{k0}, \Phi_0$ and averaged solution $\overline{\Omega}, \overline{\Sigma}, \overline{\Omega}_k, \overline{\Phi}$ have the same limit as $t \to \infty$. Setting $\Sigma = \Sigma_0 = 0$ we have similar results for the negatively curved FLRW model.

Theorem 2 applies to Bianchi III, and the invariant set $\Sigma = 0$ corresponds to negatively curved FLRW models.

$$\dot{\mathbf{x}} = H\mathbf{f}(t,\mathbf{x}) + \mathcal{O}(H^2),\ \mathbf{x} = (\Omega, \Omega_k, \Phi)^T, \tag{64}$$

$$\dot{H} = -H^2\left[\frac{1}{2}\left(3\gamma\left(1-\Omega^2-\Omega_k\right)+2\Omega_k\right)+3\Omega^2\cos^2(t\omega-\Phi)\right]+\mathcal{O}(H^3), \tag{65}$$

$$f(t,\mathbf{x}) = \begin{pmatrix} \frac{1}{2}\Omega\left(3\gamma-3\gamma\left(\Omega^2+\Omega_k\right)+2\Omega_k\right)+3\Omega\left(\Omega^2-1\right)\cos^2(t\omega-\Phi) \\ -\Omega_k\left(3\gamma\Omega^2+(3\gamma-2)(\Omega_k-1)\right)+6\Omega^2\Omega_k\cos^2(t\omega-\Phi) \\ -\frac{3}{2}\sin(2t\omega-2\Phi) \end{pmatrix}. \tag{66}$$

Replacing $\dot{\mathbf{x}} = H\mathbf{f}(t,\mathbf{x})$ with $\mathbf{f}(t,\mathbf{x})$ defined by (66) with $\dot{\mathbf{y}} = H\bar{f}(\mathbf{y})$, $\mathbf{y} = \left(\overline{\Omega}, \overline{\Omega}_k, \overline{\Phi}\right)^T$ and using the time averaging (53) we obtain the time-averaged system:

$$\dot{\overline{\Omega}} = -\frac{1}{2}H\,\overline{\Omega}\left(3(\gamma-1)\left(\overline{\Omega}^2-1\right)+(3\gamma-2)\overline{\Omega}_k\right), \tag{67}$$

$$\dot{\overline{\Omega}}_k = -H\,\overline{\Omega}_k\left(3(\gamma-1)\overline{\Omega}^2-3\gamma+(3\gamma-2)\overline{\Omega}_k+2\right), \tag{68}$$

$$\dot{\overline{\Phi}} = 0. \tag{69}$$

Universidad Católica del Norte
ver más allá

XXX CONGRESO DE MATEMÁTICA CAPRICORNIO
COMCA 2022

Point	$a(t)$	$b(t)$	Solution
T	$\frac{(3H_0t+1)}{c_2}$	$\sqrt{c_2}$	Taub-Kasner solution ($p_1 = 1, p_2 = 0, p_3 = 0$)
Q	$c_1^{-2}(3H_0t+1)^{-1/3}$	$c_1^{-1}(3H_0t+1)^{2/3}$	non-flat LRS Kasner ($p_1 = -1/3, p_2 = 2/3, p_3 = 2/3$) Bianchi I solution
D	c_1^{-1}	$\frac{(3H_0t+2)}{2\sqrt{c_1}}$	Bianchi III form of flat spacetime
F	$c_1^{-1}t^{2/3}$	$c_2^{-1/2}t^{2/3}$	Einstein-de-Sitter solution
F_0	$\ell_0\left(\frac{3\gamma H_0t}{2}+1\right)^{\frac{2}{3\gamma}}$	$\ell_0\left(\frac{3\gamma H_0t}{2}+1\right)^{\frac{2}{3\gamma}}$	Matter dominated FLRW universe
MC	$\ell_0\left(\frac{3\gamma H_0t}{2}+1\right)^{\frac{2}{3\gamma}}$	$\ell_0\left(\frac{3\gamma H_0t}{2}+1\right)^{\frac{2}{3\gamma}}$	Matter-curvature scaling solution

Point	$a(t)$	Solution
F	$a_0\left(\frac{3H_0t}{2}+1\right)^{\frac{2}{3}}$	Einstein-de-Sitter solution
F_0	$a_0\left(\frac{3\gamma H_0t}{2}+1\right)^{\frac{2}{3\gamma}}$	Matter dominated FLRW universe
C	$a_0(H_0t+1)$	Milne solution

Universidad Católica del Norte ver más allá

XXX CONGRESO DE MATEMÁTICA CAPRICORNIO COMCA 2022

Late-time behaviour: LRS Bianchi III

The results from the linear stability analysis, the Centre Manifold calculations, and combined with Theorem 2 lead to:

Theorem

The late time attractors of the full system and averaged system for Bianchi III line element are:

(i) The matter dominated FLRW universe F_0 with line element

$$ds^2 = -dt^2 + \ell_0^2 \left(\frac{3\gamma H_0 t}{2} + 1\right)^{\frac{4}{3\gamma}} \left(dr^2 + \mathbf{g}_{H^2}\right), \tag{70}$$

provided $0 < \gamma \leq 2/3$. F_0 represents a quintessence fluid for $0 < \gamma < 2/3$ or a zero-acceleration model for $\gamma = 2/3$. In the limit $\gamma = 0$, we have a de Sitter solution.

(ii) The matter-curvature scaling solution MC with $\overline{\Omega}_m = 3(1-\gamma)$ and line element (70) if $2/3 < \gamma < 1$.

(iii) The Bianchi III flat spacetime D with metric

$$ds^2 = -dt^2 + c_1^{-2} dr^2 + \frac{(3H_0 t + 2)^2}{4c_1} \mathbf{g}_{H^2}, \tag{71}$$

provided $1 \leq \gamma \leq 2$.

The results from the linear stability analysis combined with Theorem 2 (for $\Sigma = 0$) lead to:

Theorem

The late time attractors of the full system and the averaged system are:

(i) The matter dominated FLRW universe F_0 with line element

$$ds^2 = -dt^2 + a_0^2 \left(\frac{3\gamma H_0 t}{2} + 1\right)^{\frac{4}{3\gamma}} \left(dr^2 + \sinh^2(r) d\Omega^2\right), \quad (72)$$

where $d\Omega^2 = d\vartheta^2 + \sin^2\vartheta\, d\zeta^2$ is the metric for a two-sphere, provided $0 < \gamma \leq 2/3$. F_0 represents a quintessence fluid or a zero-acceleration model for $\gamma = 2/3$. In the limit $\gamma = 0$, we have a de Sitter solution.

(ii) The Milne solution C with $\overline{\Omega}_k = 1, k = -1$ with line element

$$ds^2 = -dt^2 + a_0^2 (H_0 t + 1)^2 \left(dr^2 + \sinh^2(r) d\Omega^2\right), \quad (73)$$

for $2/3 < \gamma < 2$.

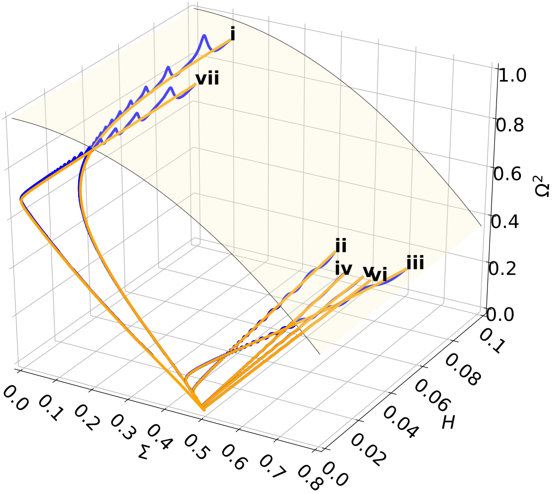

(a) Projections in the space (Σ, H, Ω^2) for the LRS Bianchi III metric when $\gamma = 1$.

Universidad Católica del Norte ver más allá

XXX CONGRESO DE MATEMÁTICA CAPRICORNIO COMCA 2022

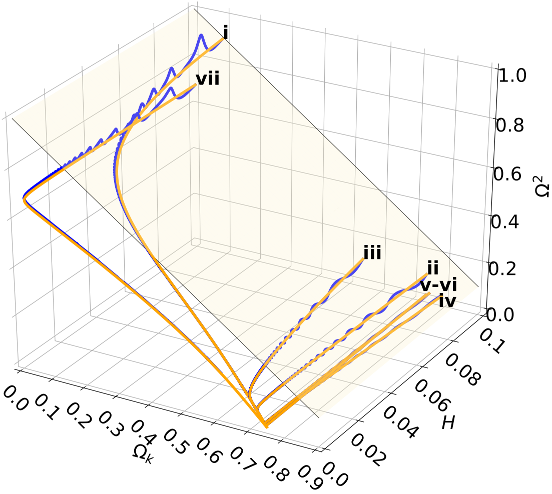

(b) Projections in the space (Ω_k, H, Ω^2) for the LRS Bianchi III metric when $\gamma = 1$.

Universidad Católica del Norte ver más allá

XXX CONGRESO DE MATEMÁTICA CAPRICORNIO COMCA 2022

62

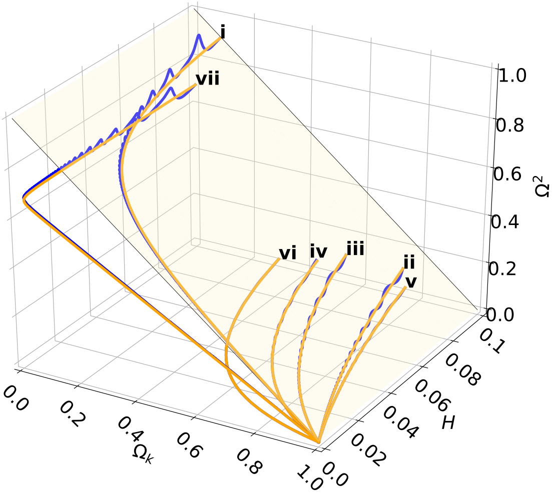

(c) Projections in the space (Ω_k, H, Ω^2) for FLRW metric with negative curvature $(k = -1)$.

Universidad Católica del Norte
ver más allá
XXX CONGRESO DE MATEMÁTICA CAPRICORNIO
COMCA 2022

- In LRS Bianchi III, late time attractors of full and averaged system are:
  (i) The matter dominated FLRW universe F_0 with line element (70) if $0 < \gamma \leq 2/3$. F_0 represents a quintessence fluid or a zero-acceleration model for $\gamma = 2/3$. In the limit $\gamma = 0$, we have the de Sitter solution.
  (ii) The matter-curvature scaling solution CS with $\bar{\Omega}_m = 3(1-\gamma)$ if $2/3 < \gamma < 1$.
  (iii) The Bianchi III flat spacetime D with line element (71) if $1 < \gamma \leq 2$.

  For FLRW metric with $k = -1$, late time attractors of full and averaged systems are:
  (i) The matter dominated FLRW universe F_0 with line element (72) for $0 < \gamma \leq 2/3$. F_0 represents a quintessence fluid or a zero-acceleration model for $\gamma = 2/3$. In the limit $\gamma = 0$, we have the de Sitter solution.
  (ii) The Milne solution C with line element (73) for $2/3 < \gamma < 2$.

  In summarising, in LRS Bianchi III, late-time attractors are a matter-dominated flat FLRW universe, a matter-curvature scaling solution, or a Bianchi III flat spacetime. FLRW metrics with $k = -1$ late time attractors are the matter-dominated FLRW universe or a Milne solution. The matter-dominated flat FLRW universe represents quintessence fluid if $0 < \gamma < 2/3$.

Universidad Católica del Norte
ver más allá
XXX CONGRESO DE MATEMÁTICA CAPRICORNIO
COMCA 2022

MUCHAS GRACIAS

1. Generalisation to 2-scalar-field theory

Now we study two canonical scalar fields ϕ_1, ϕ_2 interacting via the potential

$$V(\phi_1,\phi_2) = \mu_1^4\left[1-\cos\left(\frac{\phi_1}{f_1}\right)\right] + \mu_2^4\left[1-\cos\left(\frac{\phi_2}{f_2}\right)\right] + \mu_3^4\left[1-\cos\left(\frac{\phi_1}{f_1} - n\frac{\phi_2}{f_2}\right)\right]. \tag{74}$$

The complete action is given by $S = S_g(g_{\mu\nu}) + S_\phi(\phi_1,\phi_2) + S_m$, where S_g is the Einstein Hilbert action, S_m is the action corresponding to the non-interacting barotropic CDM and the interacting DM-DE part of the action is given by,

$$S_\phi(\phi_1,\phi_2) = -\int d^4x\sqrt{-g}\left(\frac{1}{2}(\partial\phi_1)^2 + \frac{1}{2}(\partial\phi_2)^2 + V(\phi_1,\phi_2)\right). \tag{75}$$

We get the total energy-momentum tensor consisting of the non-interacting part of the CDM and the two fields ϕ_1, ϕ_2 from the variation of $S_m + S_\phi(\phi_1,\phi_2)$ for the metric, that is, $T_{\mu\nu} = -\frac{2}{\sqrt{-g}}\frac{\delta(S_m+S_\phi)}{\delta g^{\mu\nu}}$.

Universidad Católica del Norte ver más allá

XXX CONGRESO DE MATEMÁTICA CAPRICORNIO COMCA 2022

Friedmann constraint equation is given by:

$$3H^2 = \rho + \frac{1}{2}\dot{\phi_1}^2 + \frac{1}{2}\dot{\phi_2}^2 + 2\mu_1^4 \sin^2\left(\frac{\phi_1}{2f_1}\right) + 2\mu_2^4 \sin^2\left(\frac{\phi_2}{2f_2}\right) + 2\mu_3^4 \sin^2\left(\frac{\phi_1}{2f_1} - n\frac{\phi_2}{2f_2}\right). \tag{76}$$

Raychaudhuri equation is given by:

$$2\dot{H} = -\rho - \dot{\phi_1}^2 - \dot{\phi_2}^2. \tag{77}$$

KG equations are given by:

$$\ddot{\phi_1} + 3H\dot{\phi_1} + \frac{\mu_1^4}{f_1}\sin\left(\frac{\phi_1}{f_1}\right) + \frac{\mu_3^4}{f_1}\sin\left(\frac{\phi_1}{f_1} - n\frac{\phi_2}{f_2}\right) = 0, \tag{78a}$$

$$\ddot{\phi_2} + 3H\dot{\phi_2} + \frac{\mu_2^4}{f_2}\sin\left(\frac{\phi_2}{f_2}\right) - n\frac{\mu_3^4}{f_2}\sin\left(\frac{\phi_1}{f_1} - n\frac{\phi_2}{f_2}\right) = 0. \tag{78b}$$

The continuity equation is given by:

$$\dot{\rho} + 3H\rho = 0. \tag{79}$$

Universidad Católica del Norte ver más allá

XXX CONGRESO DE MATEMÁTICA CAPRICORNIO COMCA 2022

We integrate the equations (76), (77), (78) using the redshift z instead of the cosmic time t as the independent variable. We have the differential operators:

$$\frac{df}{dt} = -H_0 E(1+z)\frac{df}{dz}, \; \frac{d^2f}{dt^2} = H_0^2 E^2 \left[(1+z)^2 \frac{d^2 f}{dz^2} + (1+z)(q+2)\frac{df}{dz}\right], \tag{80}$$

$$\frac{d^2f}{dt^2} + 3H\frac{df}{dt} = H_0^2 E^2 \left[(1+z)^2 \frac{d^2 f}{dz^2} + (1+z)(q-1)\frac{df}{dz}\right], \tag{81}$$

$$q = -1 + (1+z)\frac{d\ln H}{dz} = \frac{1}{2}\left[1 + \frac{(1+z)^2}{2}\left(\left(\frac{d\phi_1}{dz}\right)^2 + \left(\frac{d\phi_2}{dz}\right)^2\right) - \frac{V(\phi_1,\phi_2)}{E^2 H_0^2}\right]. \tag{82}$$

Hence, EQs. (78a)- (78b) becomes

$$E^2\left[(1+z)^2\frac{d^2\phi_1}{dz^2} + (1+z)(q-1)\frac{d\phi_1}{dz}\right] + \frac{\mu_1^4}{H_0^2 f_1}\sin\left(\frac{\phi_1}{f_1}\right) + \frac{\mu_3^4}{H_0^2 f_1}\sin\left(\frac{\phi_1}{f_1} - n\frac{\phi_2}{f_2}\right) = 0, \tag{83a}$$

$$E^2\left[(1+z)^2\frac{d^2\phi_1}{dz^2} + (1+z)(q-1)\frac{d\phi_1}{dz}\right] + \frac{\mu_2^4}{H_0^2 f_2}\sin\left(\frac{\phi_2}{f_2}\right) - n\frac{\mu_3^4}{f_2}\sin\left(\frac{\phi_1}{f_1} - n\frac{\phi_2}{H_0^2 f_2}\right) = 0. \tag{83b}$$

Raychaudhuri equation becomes

$$(1+z)\frac{dE}{dz} = (q+1)E. \tag{83c}$$

Universidad Católica del Norte ver más allá

XXX CONGRESO DE MATEMÁTICA CAPRICORNIO COMCA 2022

Then, we obtain a system of differential equations for $\phi_1(z)$, $\phi_2(z)$, and $E(z)$ given by (83a), (83b) and (83c) and integrate in terms of redshift z, from $z = 100$ to $z = -1$. The parameter values $f_1 = 0.1$, $f_2 = 0.1$, $\mu_1^4 = 1.1 H_0^2$, $\mu_2^4 = 10.75 H_0^2$, $\mu_3^4 = 1.07$ and $n = 9$ are chosen. As initial conditions for the fields we use $\phi_1|_{z=100} = 0.155$, $\phi_2|_{z=100} = 0.7835$, $\frac{d\phi_1}{dz}|_{z=100} = 0$ and $\frac{d\phi_2}{dz}|_{z=100} = 0$, such that $V(\phi_1(z), \phi_2(z))|_{z=100} = 11.6351 H_0^2$. As an initial condition for the Hubble parameter when $z = 100$, we take as an "educated guess" the value obtained for the ΛCDM model at $z = 100$. That is, we use the expression

$$E(z) = \sqrt{\Omega_{r0}(1+z)^4 + \Omega_{m0}(1+z)^3 + \Omega_{\Lambda 0}}, \tag{84}$$

where $\Omega_{r0} = 2.469 \times 10^{-5} h^{-2}(1 + 0.2271 N_{\text{eff}})$ and $\Omega_{\Lambda 0} = 1 - \Omega_{r0} - \Omega_{m0}$. For these parameters we consider $H_0 = 67.4\ km\ s^{-1}\ Mpc^{-1}$, $\Omega_{m0} = 0.315$ and $N_{\text{eff}} = 2.99$ according to the Planck 2018 results [N. Aghanim, *et al.*, Planck 2018].

Universidad Católica del Norte ver más allá

XXX CONGRESO DE MATEMÁTICA CAPRICORNIO COMCA 2022

For the analysis we define $\Omega_\phi = \rho_\phi / 3H^2$ and $\omega_\phi = p_\phi / \rho_\phi$, where

$$\rho_\phi = \frac{1}{2}\dot{\phi_1}^2 + \frac{1}{2}\dot{\phi_2}^2 + V(\phi_1, \phi_2),\ p_\phi = \frac{1}{2}\dot{\phi_1}^2 + \frac{1}{2}\dot{\phi_2}^2 - V(\phi_1, \phi_2), \tag{85}$$

with $V(\phi_1, \phi_2)$ given by equation (74), and from equation (76) we obtain the constraint $\Omega = 1 - \Omega_\phi$, where $\Omega = \rho / 3H^2$. We define

$$\omega_\Lambda = -1,\ r = \Omega_m / \Omega_\Lambda. \tag{86}$$

We define the kinetic and potential terms of Ω_ϕ as

$$K_1 := \frac{\dot{\phi_1}^2}{6H^2} = \frac{1}{6}(1+z)^2 \left(\frac{d\phi_1}{dz}\right)^2, \tag{87a}$$

$$K_2 := \frac{\dot{\phi_2}^2}{6H^2} = \frac{1}{6}(1+z)^2 \left(\frac{d\phi_2}{dz}\right)^2, \tag{87b}$$

$$W := \frac{V(\phi_1, \phi_2)}{3H^2} = \frac{V(\phi_1, \phi_2)}{3H_0^2 E^2}, \tag{87c}$$

$$W_{\text{int}} := \frac{\mu_3^4}{3H_0^2 E^2} \left[1 - \cos\left(\frac{\phi_1}{f_1} - n\frac{\phi_2}{f_2}\right)\right]. \tag{87d}$$

Universidad Católica del Norte ver más allá

XXX CONGRESO DE MATEMÁTICA CAPRICORNIO COMCA 2022

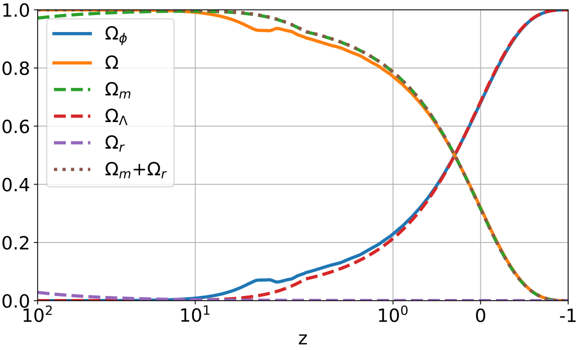

(d) Evolution of the axion-like fields density parameter Ω_ϕ and the matter density parameter Ω of our model and the density parameters Ω_m, Ω_Λ and Ω_r of ΛCDM as a function of the redshift z.

Universidad Católica del Norte
ver más allá

XXX CONGRESO DE MATEMÁTICA CAPRICORNIO
COMCA 2022

72

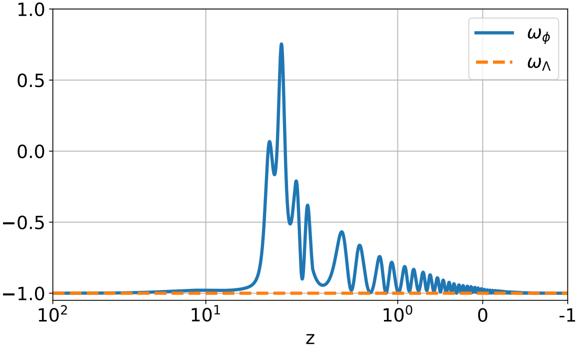

(e) Evolution of the effective barotropic index ω_ϕ associated to the axion-like fields as a function of the redshift z and $\omega_\Lambda = -1$ corresponding to ΛCDM.

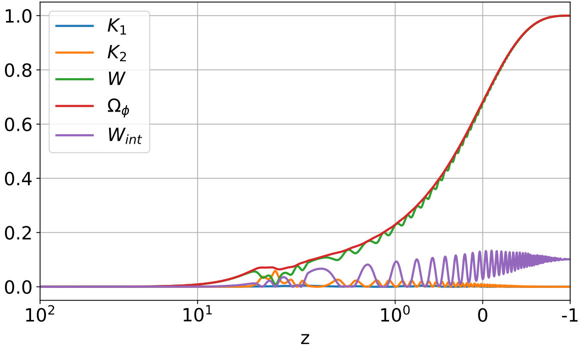

(f) Evolution of the kinetic, potential and interaction terms of Ω_ϕ given by (87) as functions of redshift z.

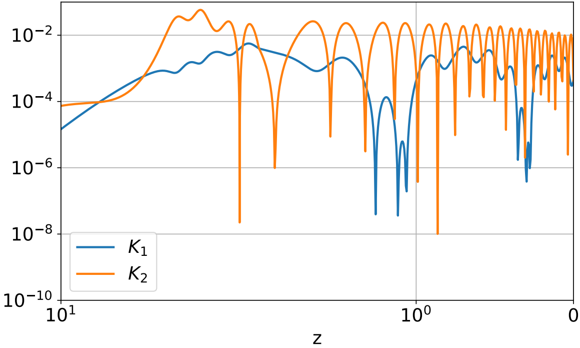

(g) Zoom of kinetic terms (87a) and (87b) as functions of redshift z.

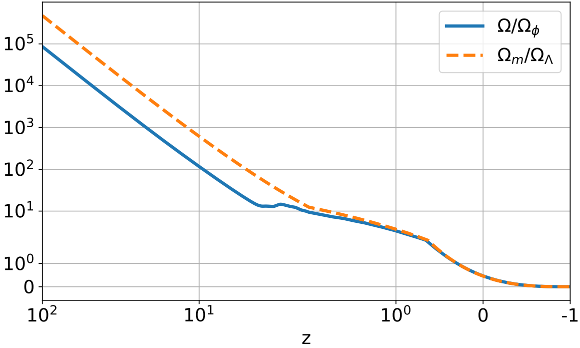

(h) Evolution of the ratios Ω/Ω_ϕ and Ω/Ω_Λ as a function of the redshift z. According Planck 2018 results [N. Aghanim, *et al.*, Planck 2018], the current value of r is $\Omega_{m0}/\Omega_{\Lambda_0} = 63/137$.

Universidad Católica del Norte
ver más allá
XXX CONGRESO DE MATEMÁTICA CAPRICORNIO
COMCA 2022

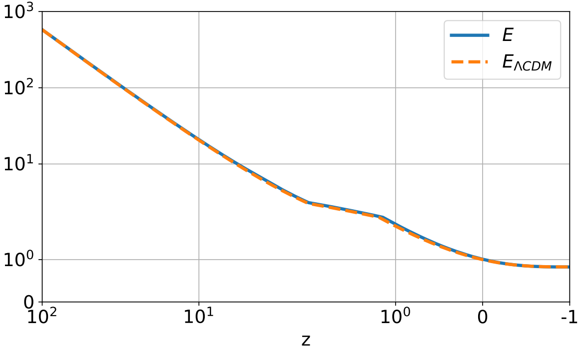

(i) Evolution of the dimensionless Hubble parameter $E = H/H_0$ for our model and for ΛCDM as a function of the redshift z.

Universidad Católica del Norte
ver más allá
XXX CONGRESO DE MATEMÁTICA CAPRICORNIO
COMCA 2022

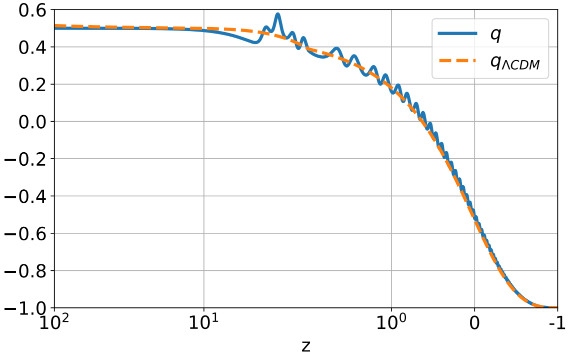

(j) Evolution of the deceleration parameter defined by $q := -1 - \dot{H}/H^2$ for our model and for ΛCDM as a function of the redshift z.

Universidad Católica del Norte
ver más allá
XXX CONGRESO DE MATEMÁTICA CAPRICORNIO
COMCA 2022

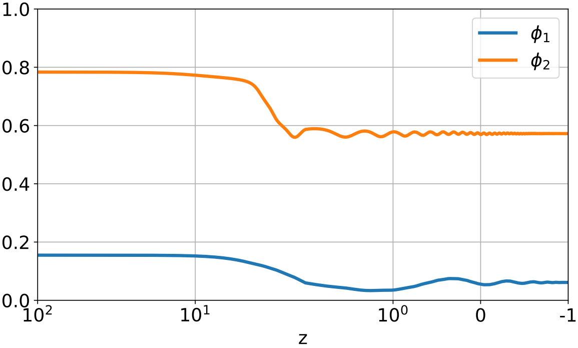

(k) Evolution of the axion-like fields ϕ_1 and ϕ_2 as a function of the redshift z.

Figure: Numerical simulation of the system (77)-(78) with initial conditions $\phi_1|_{z=100} = 0.155$, $\phi_2|_{z=100} = 0.7835$, $\frac{d\phi_1}{dz}_{z=100} = 0$ and $\frac{d\phi_2}{dz}_{z=100} = 0$. The initial value $H|_{z=100}$ is estimated from expression (84). The exact solutions for the ΛCDM model are superimposed for comparison.

Universidad Católica del Norte ver más allá
XXX CONGRESO DE MATEMÁTICA CAPRICORNIO COMCA 2022

79

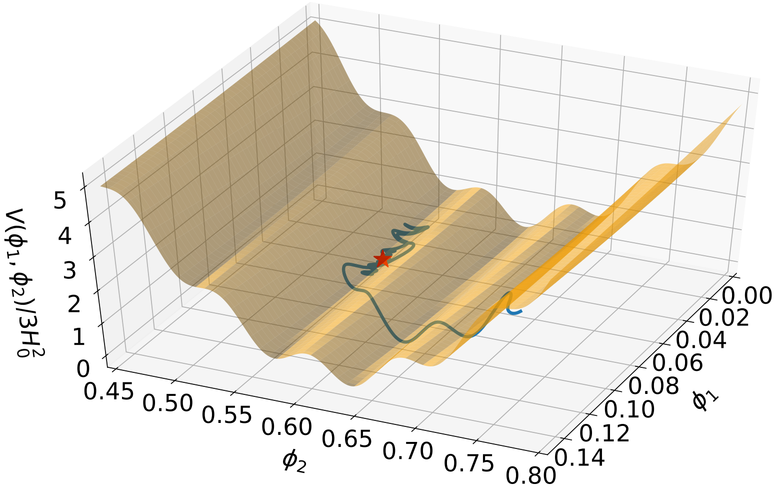

(a) Surface $V(\phi_1, \phi_2)/(3H_0^2)$.

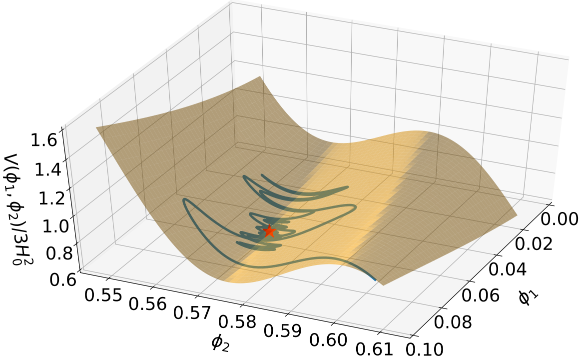

(b) Surface $V(\phi_1, \phi_2)/(3H_0^2)$ (basin of attraction of ϕ^*).

Figure: Surface $V(\phi_1, \phi_2)/(3H_0^2)$ with the local minimum of $V(\phi_1, \phi_2)/(3H_0^2)$ at $\phi^* := (\phi_1, \phi_2) = (0.0614165, 0.572375)$ with minimum value of $\frac{\Lambda_{\text{eff}}}{3H_0^2} = 0.682603$ (denoted by a red star). The parametric curve (denoted by a blue line) $\frac{V(\phi_1(z),\phi_2(z))}{3H_0^2}, z \in [-1, 100]$, obtained by evaluating the solution which converges to ϕ^*, is attached to the surface.

Universidad Católica del Norte
ver más allá
XXX CONGRESO DE MATEMÁTICA CAPRICORNIO
COMCA 2022

Let us assume $n \neq 0$. Defining the new fields

$$\Psi_1 = \sqrt{\frac{c^2}{1+c^2}}\left(\phi_2 - \frac{\phi_1}{c}\right), \; \Psi_2 = \sqrt{\frac{1}{1+c^2}}\left(c\phi_1 + \phi_2\right), \tag{88}$$

the field equations become

$$\ddot{\Psi}_1 + 3H\dot{\Psi}_1 = f_1(\Psi_1, \Psi_2; a_i, b_j, c, n, H_0^2), \tag{89a}$$

$$\ddot{\Psi}_2 + 3H\dot{\Psi}_2 = f_2(\Psi_1, \Psi_2; a_i, b_j, c, n, H_0^2), \tag{89b}$$

$$3H^2 - U(\Psi_1, \Psi_2; a_i, b_j, c, n, H_0^2) - \rho - \frac{1}{2}\dot{\Psi}_1{}^2 - \frac{1}{2}\dot{\Psi}_2{}^2 = 0. \tag{89c}$$

Universidad Católica del Norte ver más allá

XXX CONGRESO DE MATEMÁTICA CAPRICORNIO COMCA 2022

82

Imposing the conditions

$$c=\frac{3a_1\left(b_2+2b_3n^2\right)-6a_2(b_1+b_3)+\sqrt{\left(6a_2(b_1+b_3)-3a_1\left(b_2+2b_3n^2\right)\right)^2+144a_1a_2b_3^2n^2}}{12\sqrt{a_1}\sqrt{a_2}b_3n}, \tag{90a}$$

$$\frac{\omega_1}{H_0}=\frac{\sqrt{a_1\left(b_2+2b_3n^2\right)+2a_2(b_1+b_3)+\sqrt{4a_1^2b_3^2n^4+4a_1b_3n^2(a_1b_2-2a_2b_1+2a_2b_3)+(a_1b_2-2a_2(b_1+b_3))^2}}}{2\sqrt{a_1}\sqrt{a_2}}, \tag{90b}$$

$$\frac{\omega_2}{H_0}=\frac{\sqrt{a_1\left(b_2+2b_3n^2\right)+2a_2(b_1+b_3)-\sqrt{4a_1^2b_3^2n^4+4a_1b_3n^2(a_1b_2-2a_2b_1+2a_2b_3)+(a_1b_2-2a_2(b_1+b_3))^2}}}{2\sqrt{a_1}\sqrt{a_2}}, \tag{90c}$$

we obtain the decoupled oscillators

$$\ddot{\Psi}_1+3H\dot{\Psi}_1+\omega_1^2\Psi_1=0,\ \ddot{\Psi}_2+3H\dot{\Psi}_2+\omega_2^2\Psi_2=0 \tag{91}$$

in the limit $\Psi_i \to 0$. Therefore, as $H \to 0$, we obtain the decoupled oscillators

$$\ddot{\Psi}_1+\omega_1^2\Psi_1=0,\ \ddot{\Psi}_2+\omega_2^2\Psi_2=0. \tag{92}$$

The solutions of (92) can be written as

$$\Psi_i(t)=r_i\sin\left(t\omega_i-\Phi_i\right),\ \dot{\Psi}_1(t)=r_i\omega_i\cos\left(t\omega_i-\Phi_i\right),i=1,2, \tag{93}$$

where r_i and Φ_i are integration constants.

Universidad Católica del Norte ver más allá
XXX CONGRESO DE MATEMÁTICA CAPRICORNIO COMCA 2022

According to the Raychaudhuri equation (77), H is a monotonic decreasing function. Additionally, as the minimum of $V(\phi_1, \phi_2)$ in $(\phi_1, \phi_2) = (0, 0)$ is approached, $H \to 0$. Therefore, as $H \to 0$, we obtain the decoupled oscillators (92). Motivated by the solution (93), we use the variation of constants to propose the solution of the full KG system as

$$\Psi_i(t) = r_i(t) \sin\left(t\omega_i - \Phi_i(t)\right), \; \dot{\Psi}_i = r_i(t)\omega_i \cos\left(t\omega_i - \Phi_i(t)\right), i = 1, 2, \tag{94a}$$

with inverse functions

$$r_i = \sqrt{\Psi_i^2 + \left(\frac{\dot{\Psi}_i}{\omega_i}\right)^2}, \; \Phi_i = t\omega_i - \tan^{-1}\left(\frac{\omega_i \Psi_i}{\dot{\Psi}_i}\right), i = 1, 2, \tag{95}$$

where c and ω_1, ω_2 are undetermined constants. Let us define

$$\Omega_i = \frac{r_i^2 \omega_i}{6H^2}, \; \Omega = \frac{\rho}{3H^2}. \tag{96}$$

Universidad Católica del Norte ver más allá

XXX CONGRESO DE MATEMÁTICA CAPRICORNIO COMCA 2022

By expanding in Taylor's series around $H=0$, we have the 6- dimensional system

$$\dot{x} = HF^{[1]}(t,x) + \mathcal{O}\left(H^2\right),\ x(0)=x_0,\ t\geq 0, \tag{97a}$$

$$\dot{H} = -G^{[2]}(t,x)H^2, \tag{97b}$$

where

$$x = \left(\Omega_1, \Omega_2, \Omega, \Phi_1, \Phi_2\right)^T, \tag{98}$$

$$G^{[2]}(t,x) = 3\Omega_1\cos^2(\Phi_1 - t\omega_1) + 3\Omega_2\cos^2(\Phi_2 - t\omega_2) + \frac{3\Omega}{2}, \tag{99}$$

and

$$F^{[1]}(t,x) = \begin{pmatrix} 3\Omega_1\left(2(\Omega_1-1)\cos^2(t\omega_1-\Phi_1) + 2\Omega_2\cos^2(t\omega_2-\Phi_2)+\Omega\right) \\ 3\Omega_2\left(2\Omega_1\cos^2(t\omega_1-\Phi_1) + 2(\Omega_2-1)\cos^2(t\omega_2-\Phi_2)+\Omega\right) \\ 3\Omega(\Omega+\Omega_1+\Omega_2+\Omega_1\cos(2(t\omega_1-\Phi_1))+\Omega_2\cos(2(t\omega_2-\Phi_2))-1) \\ -\frac{3}{2}\sin(2(t\omega_1-\Phi_1)) \\ -\frac{3}{2}\sin(2(t\omega_2-\Phi_2)) \end{pmatrix}. \tag{100}$$

time averaging

If we have vector functions $f_n(t,x)$ which have N independent periods $T_n,\ n=1,\ldots,N$, Take the averaging

$$\dot{y} = \varepsilon f^{(0)}(y),\ y(0) = x_0,\ f^{(0)}(y) = \sum_{n=1}^{N} \frac{1}{T_n} \int_0^{T_n} f_n(t,y)dt, \tag{101}$$

where y is considered a parameter kept constant during integration. Assuming $\omega_1 \neq \omega_2$, with H playing the role of ε, $N=2$, $T_1 = \frac{2\pi}{\omega_1}$ and $T_2 = \frac{2\pi}{\omega_2}$ we can use the following averaging procedure:

$$f^{(0)}(y) = \frac{\omega_1}{2\pi} \int_0^{\frac{2\pi}{\omega_1}} f_1(t,y)dt + \frac{\omega_2}{2\pi} \int_0^{\frac{2\pi}{\omega_2}} f_2(t,y)dt \tag{102}$$

where the vector field $f(t,y)$ in the right-hand-side of the equation must be the sum of two vector functions $f_1(t,y)$ and $f_2(t,y)$ where each of them is periodic with one period. The averaged system obtained using such an approach is

$$\begin{pmatrix} \partial_t\overline{\Omega}_1 \\ \partial_t\overline{\Omega}_2 \\ \partial_t\overline{\Omega} \\ \partial_t\overline{\Phi}_1 \\ \partial_t\overline{\Phi}_2 \end{pmatrix} = -3H \begin{pmatrix} \overline{\Omega}_1\left(1-\overline{\Omega}_1-\overline{\Omega}_2-\overline{\Omega}\right) \\ \overline{\Omega}_2\left(1-\overline{\Omega}_1-\overline{\Omega}_2-\overline{\Omega}\right) \\ \overline{\Omega}\left(1-\overline{\Omega}_1-\overline{\Omega}_2-\overline{\Omega}\right) \\ 0 \\ 0 \end{pmatrix}, \tag{103a}$$

$$\dot{H} = -\frac{3}{2}H^2\left(\overline{\Omega}_1+\overline{\Omega}_2+\overline{\Omega}\right). \tag{103b}$$

We implement a local nonlinear transformation:

$$\mathbf{x}_0 := (\Omega_{10}, \Omega_{20}, \Omega_0, \Phi_{10}, \Phi_{20})^T \mapsto \mathbf{x} := (\Omega_1, \Omega_2, \Omega, \Phi_1, \Phi_2)^T$$

$$\mathbf{x} = \psi(\mathbf{x}_0) := \mathbf{x}_0 + H\mathbf{g}(H, \mathbf{x}_0, t), \; \mathbf{g}(H, \mathbf{x}_0, t) = \begin{pmatrix} g_1(H, \Omega_{10}, \Omega_{20}, \Omega_0, \Phi_{10}, \Phi_{20}, t) \\ g_2(H, \Omega_{10}, \Omega_{20}, \Omega_0, \Phi_{10}, \Phi_{20}, t) \\ g_3(H, \Omega_{10}, \Omega_{20}, \Omega_0, \Phi_{10}, \Phi_{20}, t) \\ g_4(H, \Omega_{10}, \Omega_{20}, \Omega_0, \Phi_{10}, \Phi_{20}, t) \\ g_5(H, \Omega_{10}, \Omega_{20}, \Omega_0, \Phi_{10}, \Phi_{20}, t) \end{pmatrix}. \quad (104)$$

Theorem

Let $\overline{\Omega}_1, \overline{\Omega}_2, \overline{\Omega}, \overline{\Phi}_1, \overline{\Phi}_2$. Furthermore, H be defined functions that satisfy averaged equations (103). Then, there exist continuously differentiable functions g_1, g_2, g_3, g_4 and g_5, such that $\Omega_1, \Omega_2, \Omega, \Phi_1, \Phi_2$ are locally given by (104), where $\Omega_{10}, \Omega_{20}, \Omega_0, \Phi_{10}, \Phi_{20}$ are order zero approximations of them as $H \to 0$. Then, functions $\Omega_{10}, \Omega_{20}, \Omega_0, \Phi_{10}, \Phi_{20}$ and averaged solution $\overline{\Omega}_1, \overline{\Omega}_2, \overline{\Omega}, \overline{\Phi}_1, \overline{\Phi}_2$ have the same limit as $t \to \infty$.

Theorem 5 implies that $\Omega_i, \Omega, \Phi_i, i = 1, 2$ evolves according to the averaged equations (103) as $H \to 0$.

1. The perturbed system truncated at second order in H:

$$
\begin{cases}
\frac{dH}{d\tau} = -H\left[3\Omega_1\cos^2(t\omega_1-\Phi_1)+3\Omega_2\cos^2(t\omega_2-\Phi_2)+\frac{3\Omega}{2}\right],\ \frac{dt}{d\tau}=1/H,\\
\frac{d\Omega_1}{d\tau} = 3\Omega_1\left(2(\Omega_1-1)\cos^2(t\omega_1-\Phi_1)+2\Omega_2\cos^2(t\omega_2-\Phi_2)+\Omega\right),\\
\frac{d\Omega_2}{d\tau} = 3\Omega_2\left(2\Omega_1\cos^2(t\omega_1-\Phi_1)+2(\Omega_2-1)\cos^2(t\omega_2-\Phi_2)+\Omega\right),\\
\frac{d\Omega}{d\tau} = 3\Omega(\Omega+\Omega_1+\Omega_2+\Omega_1\cos(2(t\omega_1-\Phi_1))+\Omega_2\cos(2(t\omega_2-\Phi_2))-1),\\
\frac{d\Phi_1}{d\tau} = -\frac{3}{2}\sin(2(t\omega_1-\Phi_1)),\ \frac{d\Phi_2}{d\tau} = -\frac{3}{2}\sin(2(t\omega_2-\Phi_2)).
\end{cases}
\tag{105}
$$

2. The averaged system:

$$
\begin{cases}
\frac{dH}{d\tau} = -\frac{3}{2}H\left(\overline{\Omega}_1+\overline{\Omega}_2+\overline{\Omega}\right),\ \frac{dt}{d\tau}=1/H,\\
\frac{d\overline{\Omega}_1}{d\tau} = -3\overline{\Omega}_1\left(1-\overline{\Omega}_1-\overline{\Omega}_2-\overline{\Omega}\right),\\
\frac{d\overline{\Omega}_2}{d\tau} = -3\overline{\Omega}_2\left(1-\overline{\Omega}_1-\overline{\Omega}_2-\overline{\Omega}\right),\\
\frac{d\overline{\Omega}}{d\tau} = -3\overline{\Omega}\left(1-\overline{\Omega}_1-\overline{\Omega}_2-\overline{\Omega}\right),\\
\frac{d\overline{\Phi}_1}{d\tau} = 0,\ \frac{d\overline{\Phi}_1}{d\tau} = 0.
\end{cases}
\tag{106}
$$

Universidad Católica del Norte ver más allá

XXX CONGRESO DE MATEMÁTICA CAPRICORNIO COMCA 2022

Table: Five initial data sets for the simulation of the truncated system (105) and time-averaged system (106). All the conditions are chosen in order to fulfil the inequality $\overline{\Omega}_1 + \overline{\Omega}_2 + \overline{\Omega} \leq 1$.

Sol.	$H(0)$	$\overline{\Omega}_1(0)$	$\overline{\Omega}_2(0)$	$\overline{\Omega}(0)$	$\overline{\Phi}_1(0)$	$\overline{\Phi}_2(0)$	$t(0)$
i	0.01	0.255	0.255	0.113	0	0	0
ii	0.1	0.424	0.261	0.315	0	0	0
iii	0.1	0.243	0.342	0.315	0	0	0
iv	0.1	0.105	0.178	0.526	0	0	0
v	0.1	0.005	0.078	0.786	0	0	0

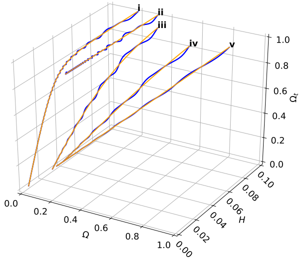

(a) Projections in the space (Ω, H, Ω_t), where $\Omega_t = \Omega_1 + \Omega_2 + \Omega$.

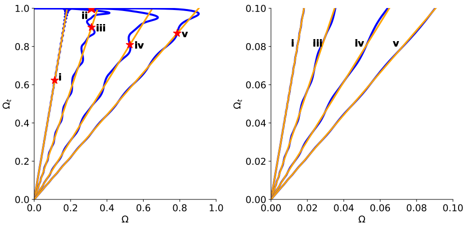

(b) Projections in the space (Ω, Ω_t), where $\Omega_t = \Omega_1 + \Omega_2 + \Omega$. The plot on the right represents a zoomed region of the plot on the left.

Figure: Some solutions of the truncated system (105) (blue) and time-averaging system (106) (orange) for the fixed values of $\omega_1 = \sqrt{2}$ and $\omega_2 = \sqrt{2}/2$. We use the five data sets presented in Table 3 as initial conditions for both systems. These plots are numerical evidence that the main theorem 5 is fulfilled. That is, the solution of the truncated system follows the track of the solutions of the time-averaged system and the oscillations experimented by the truncated system are smoothed out as $H \to 0$.

1. We have analysed several cosmological models, and we finalised a model consisting of two canonical scalar fields ϕ_1, ϕ_2 interacting via the potential. We have introduced dimensionless dynamical variables and dimensionless time variables.
2. In the first-order approximations of matter, normalised scalar field densities and the values of two scalar fields Φ_1 and Φ_2 (which are functions of ϕ_1 and ϕ_2) as $H \to 0$ and their averaged values –with a properly defined averaging process– have the same limit as $H \to 0$ (as $\tau \to \infty$). That was summarised in theorem 5.
3. Therefore, with this approach, oscillations entering the nonlinear system through the KG equation can be controlled and smoothed out as the Hubble factor H, acting as a time-dependent perturbation parameter, tends monotonically to zero.
4. We have studied the time-averaged system using standard techniques of dynamical systems and presented numerical simulations as evidence of such behaviour.

Universidad Católica del Norte
ver más allá
XXX CONGRESO DE MATEMÁTICA CAPRICORNIO
COMCA 2022

1. This approach is helpful to describe inflaton's oscillations around the potential minimum during reheating after inflation. For nonzero H, this gives rise to time-dependent oscillatory dynamics. That is responsible for particle production via quantum field theory.
2. The relevant calculations depend on the form of the potential and, in particular, are pretty complicated for harmonic potentials. The result here shows that one can "average out" the oscillations arising from the harmonic functions, thus simplifying the problem. Indeed, by using some inverse transformations, one can find from the $\overline{\Omega}_i$ to $\overline{\Phi}_i$, i.e., the averaged version of the original field variables. We hope this approach may help reheat calculations in the N-inflation model.
3. This approach is also suitable in the linear cosmological perturbations context. In the cosmological perturbation theory, cosmological perturbations at the linear level are governed by equations whose coefficients are composed of background quantities; therefore, proper knowledge of the background dynamics is necessary for further perturbation analyses.

THANK YOU FOR YOUR ATTENTION

- Wainwright, J., & Ellis, G. (Eds.) (1997). Dynamical Systems in Cosmology. Cambridge: Cambridge University Press. doi:10.1017/CBO9780511524660.
- Coley, A.A. (2003) Dynamical systems and cosmology. Dordrecht, The Netherlands: Springer-Science+Business Media, B.V. doi: 10.1007/978-94-017-0327-7.
- PERKO, L. Differential equations and dynamical systems, third edition. Springer-Verlag, New York, 2001
- Sanders J., Verhulst F., Murdock, J., Averaging Methods in Nonlinear Dynamical Systems (Applied Mathematical Sciences vol 59, Springer Science + Business Media, LLC, 2010) 2nd edn (Berlin).
- D. Fajman, G. Heißel and M. Maliborski, Class. Quant. Grav. **37** (2020) no.13, 135009
- D. Fajman, G. Heißel and J. W. Jang, Class. Quant. Grav. **38** (2021) no.8, 085005
- N. Aghanim *et al.* [Planck], Astron. Astrophys. **641** (2020), A6 doi:10.1051/0004-6361/201833910